GEOLOGIC MAP OF THE SEABECK AND POULSBO 7.5-MINUTE QUADRANGLES, KITSAP AND JEFFERSON COUNTIES, WASHINGTON

by Michael Polenz, Gary T. Petro,
Trevor A. Contreras, Kimberly A. Stone,
Gabriel Legorreta Paulin, and Recep Cakir

WASHINGTON
DIVISION OF GEOLOGY
AND EARTH RESOURCES
Map Series 2013-02
October 2013

WASHINGTON STATE DEPARTMENT OF
Natural Resources
Peter Goldmark - Commissioner of Public Lands

DISCLAIMER

INDEMNIFICATION

Research supported by the U.S. Geological Survey, National Cooperative Geologic Mapping Program, under USGS award number G12AC20234. The views and conclusions contained in this document are those of the authors and should not be interpreted as necessarily representing the official policies, either expressed or implied, of the U.S. Government.

WASHINGTON STATE DEPARTMENT OF NATURAL RESOURCES

DIVISION OF GEOLOGY AND EARTH RESOURCES

Washington Department of Natural Resources
Division of Geology and Earth Resources

Mailing Address:
MS 47007
Olympia, WA 98504-7007

Street Address:
Natural Resources Bldg, Rm 148
1111 Washington St SE
Olympia, WA 98501

Phone: 360-902-1450; *Fax:* 360-902-1785
E-mail: geology@dnr.wa.gov
Website: http://www.dnr.wa.gov/geology

This and other DGER publications are available online at:
http://www.dnr.wa.gov/Publications/ger_publications_list.pdf

The online catalog of the Washington Geology Library is at:
http://www.dnr.wa.gov/ResearchScience/Topics/GeologyPublications Library/Pages/washbib.aspx

Washington State Geologic Information Portal:
http://www.dnr.wa.gov/geologyportal

Suggested Citation: Polenz, Michael; Petro, G. T.; Contreras, T. A.; Stone, K. A.; Legorreta Paulin, Gabriel; Cakir, Recep, 2013, Geologic map of the Seabeck and Poulsbo 7.5-minute quadrangles, Kitsap and Jefferson Counties, Washington: Washington Division of Geology and Earth Resources Map Series 2013-02, 1 sheet, scale 1:24,000, with 39 p. text.

Published in the United States of America

Table of Contents

Introduction 1
Geologic Setting 1
  Tectonic Framework 1
  Landscape Development 4
    Pre-Vashon Sediment 4
    Vashon Drift 5
  Quaternary Structure and Neotectonics 7
    Seattle Fault 7
    Dabob Bay Fault Zone 8
    Apex Anticline 10
    Anderson Creek Syncline 11
    Other Observations with Potential Structural Significance 11
Description of Map Units 11
  Quaternary Unconsolidated Deposits 12
    Holocene Nonglacial Deposits 12
    Latest Pleistocene to Holocene Nonglacial Deposits 12
    Pleistocene Glacial and Nonglacial Deposits 14
      Vashon Drift (northern-sourced) 14
      Pre-Vashon Glacial Deposits 18
        Pre-Vashon Olympic-Sourced Glacial Deposits 18
        Pre-Vashon Northern-Sourced Glacial Deposits 19
        Pre-Vashon Nonglacial Deposits 21
      Glacial and Nonglacial Deposits, Undivided 22
  Tertiary Sedimentary and Volcanic Bedrock 23
Acknowledgments 23
References Cited 24
Appendix A. Bedrock Elevation Estimates from Passive Seismic Survey Data 29
Appendix B. New Radiocarbon and Luminescence Dates 31
Appendix C. New Tephra Data from Geochemistry Site G1 35
Appendix D. Illustrations of Selected Field Sites 36

List of Figures

Figure 1. Shaded relief map of regional structure in the report area 2

Figure 2. Harding diagrams for dextral transpression 3

Figure 3. Comparison of geologic time scale, global magnetic polarity, marine oxygen isotope curve and stages, and ages of climatic intervals in the Puget and Fraser Lowland 5

Figure 4. Equal-angle stereonet plots of fold axes of deformed Pleistocene strata. 8

Figure 5. Site S2, folded and faulted nonglacial deposits at Dabob Bay fault 5 (sec. 28, T26N R1W) 10

Figure D1. Aerial photograph showing the location of the relict peat and tree stump at date site GD1 (sec. 21, T25N R1E, east shore of Dyes Inlet) 36

Figure D2. Photographs of rhythmically bedded sand of unit Qgos with slump structures in the main pit wall of Asbury's Topsoil sand pit and in a subpit of the main pit floor 37

Figure D3. Photograph of planar to gently crossbedded sand with pebble lenses of unit Qpos in the cutbank of a ravine at the southern edge of the Poulsbo quadrangle west of Dyes Inlet 38

Figure D4. Photograph of gently folded and fractured, planar-bedded, pebbly sand and silt of unit Qc_O along a bluff on the east shore of Dyes Inlet 39

List of Tables

Table 1. Elevation ranges for clusters of relict shorelines 6

Table A1. Bedrock elevation estimates 29

Table B1. Radiocarbon age-control data from the map area 31

Table B2. Infrared and optically stimulated luminescence age-control results from the map area 33

Table B3. Luminescence analytical data for age-control results from the map area 34

Table C1. New electron microprobe geochemical data on tephra at geochemistry site G1 (unit Qoa) 34

Map Sheet

Geologic map of the Seabeck and Poulsbo 7.5-minute quadrangles, Kitsap and Jefferson Counties, Washington

Geologic Map of the Seabeck and Poulsbo 7.5-minute Quadrangles, Kitsap and Jefferson Counties, Washington

by Michael Polenz[1], Gary T. Petro[1], Trevor A. Contreras[1], Kimberly A. Stone[1], Gabriel Legorreta Paulin[2], Recep Cakir[1]

[1] Washington Division of Geology and Earth Resources
MS 47007
Olympia, WA 98504-7007

[2] Universidad Nacional Autónoma de México
Instituto de Geografía
Ciudad Universitaria, Del Coyoacán
cp 04510, México, D.F.

INTRODUCTION

This pamphlet provides unit descriptions, interpretations, and data for the accompanying geologic map sheet for the Seabeck and Poulsbo quadrangles, which straddle Hood Canal in the Puget Lowland. The Seabeck–Poulsbo map is part of a systematic effort to develop 1:24,000-scale geologic maps along all of Hood Canal, an increasingly populated, strategically important, geologically active, and ecologically sensitive region. Our map and cross sections build on previous mapping (Grimstad and Carson, 1981; Yount and Gower, 1991; Yount and others, 1993; Deeter, 1979, and unpub. field notes; Birdseye, 1976; Kahle, 1998; Haugerud, 2009) by adding detailed field observations and new geological analyses. We incorporate review of hundreds of well records, boring records, and geotechnical reports from multiple sources (Wash. Dept. of Ecology [WADOE]; U.S. Geological Survey [USGS]; Kitsap County; Wash. Dept. of Transportation [WSDOT]; Robinson Noble, Inc.; City of Poulsbo). Appendix A presents bedrock elevation estimates that we developed from passive seismic survey data, Appendix B presents new radiocarbon and luminescence dates, Appendix C presents tephra data, and Appendix D presents photographs of selected sites.

GEOLOGIC SETTING

Tectonic Framework

The map area is in the Cascadia subduction zone forearc, where oblique convergence causes active structures to accommodate margin-parallel shortening (Johnson and others, 2004). The map area is bounded to the south by the active Seattle fault zone (Kimball, 1897; Raisz, 1945; Daneš and others, 1965; Gower and others, 1985; Bucknam and others, 1992; Blakely and others, 2002; Brocher and others, 2004; Kelsey and others, 2008; Tabor and others, 2011; Lamb and others, 2012) and straddles the transition from the Seattle basin on the east to the Olympic Mountains on the west (Fig. 1). The Hood Canal fault has been inferred along this transition (Daneš and others, 1965; Gower and others, 1985), but in the map area the transition is structurally complex with multiple faults and structures that are not necessarily explained by the meeting of the Seattle and Hood Canal faults—a notion also reinforced by Mace and Keranen (2012), who pointed out that much of the crustal seismicity beneath the Puget Lowland, including our map area, is not explained by known structures. If the Hood Canal fault traverses the map area, we do not know where and to what local effect. To the northeast of the map area is the northwest-trending, right-lateral, transpressional southern Whidbey Island fault zone, which accommodates margin-parallel transport of southwestern Washington relative to North America (Johnson and others, 1996; Sherrod and others, 2008; Blakely and others, 2011).

Tomographic modeling (Van Wagoner and others, 2002; Brocher and others, 2001) suggests that the map area marks the western limit of the Seattle basin. Previous mapping (Kahle, 1998), well and boring records, and total-field and residual aeromagnetic and gravitational field strength data (aeromagnetic data not reduced to pole)(Richard Blakely, USGS, written commun., 2012, 2013) are consistent with that interpretation. We verified bedrock depth by reviewing hundreds of geotechnical and well records and using passive seismic data

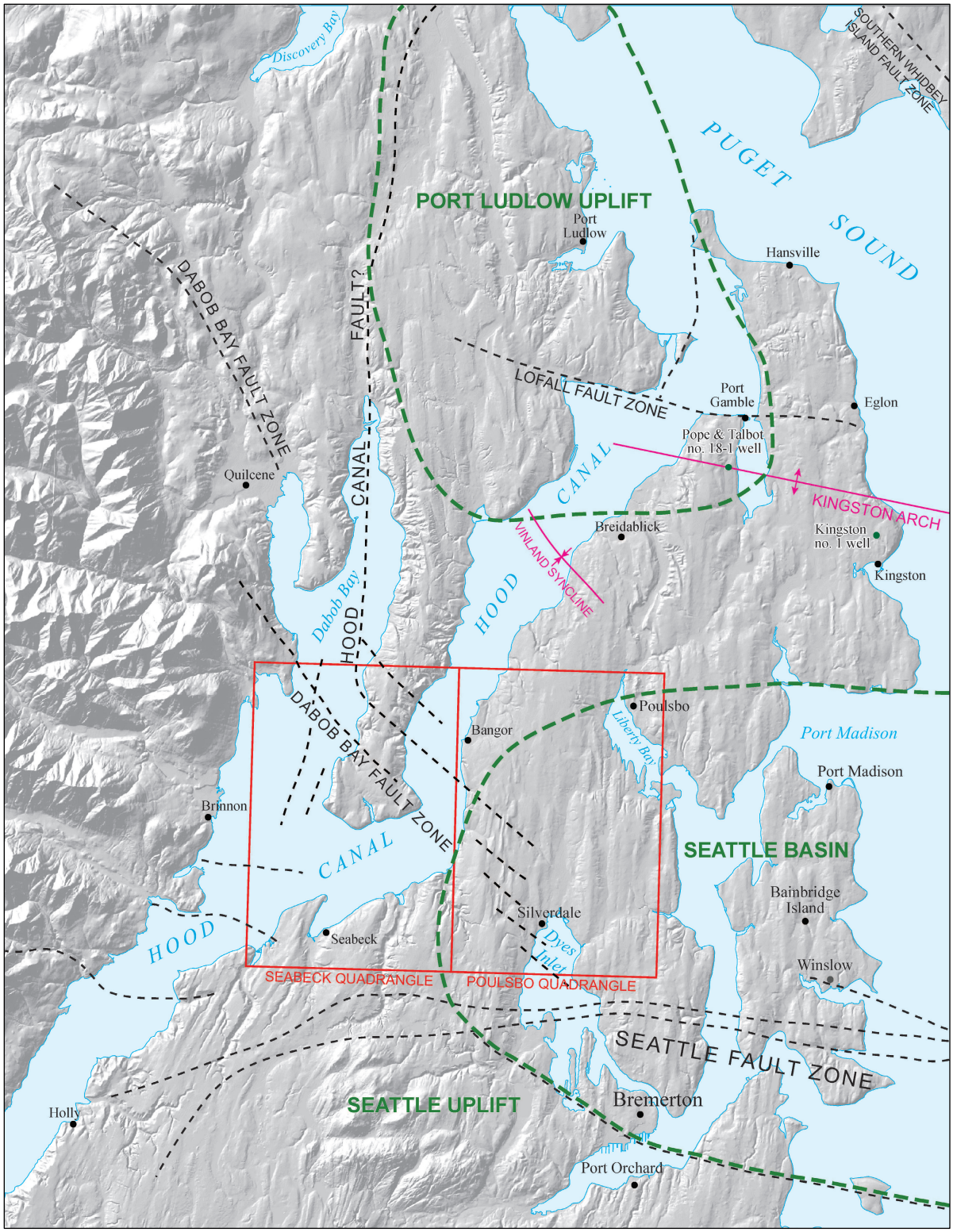

Figure 1. Shaded relief map of regional structure in the report area. Faults in and adjacent to the quadrangles (red rectangles) are shown as indicated by current field investigations (Contreras and others, 2013; Polenz and others, 2013), while regional faults were redrawn from previous investigations (Lamb and others, 2012; Blakely and others, 2009; active faults layer of the Washington Interactive Geologic Map, accessed May 2013 on the Washington State Geologic Information Portal at http://www.dnr.wa.gov/geologyportal). Geophysical studies (Pratt and others, 1997) provided the information on uplifts and basins.

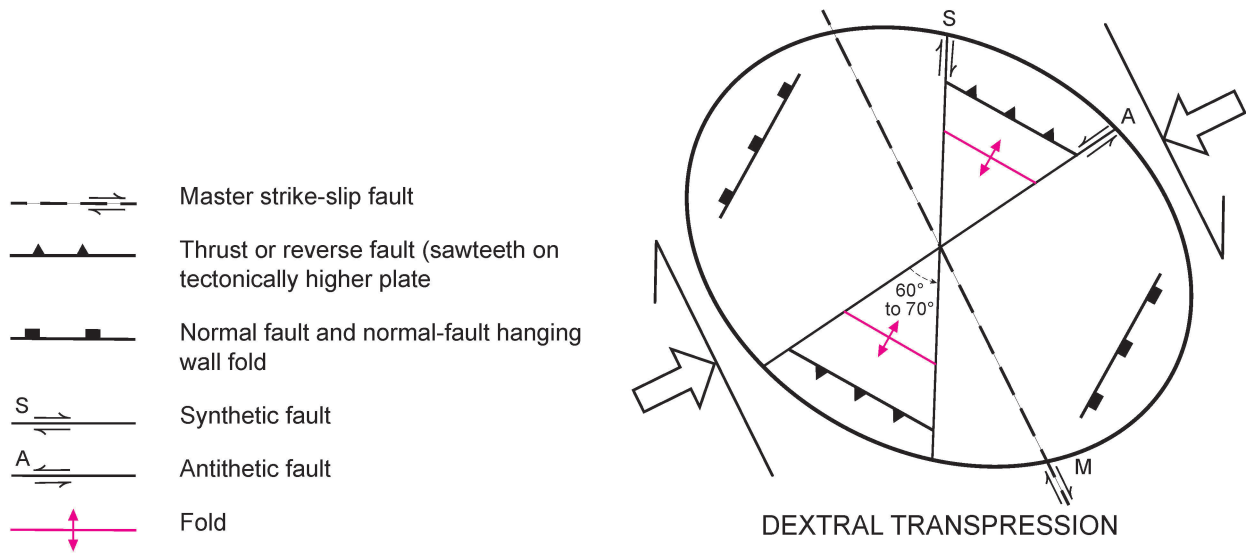

Figure 2. Harding diagram for dextral transpression. The diagram shows forces and a composite of structures (normal faults and normal fault-parallel hanging-wall folds, thrust or reverse faults and folds, synthetic and antithetic faults) that can result from wrenching deformation. To approximate orientations of structures observed in the map area, the diagram is oriented as if the master strike-slip structure was the southern Whidbey Island fault zone. Revised from Harding (1974) and Sanderson and Marchini (1984).

to estimate depth to bedrock at HVSR (horizontal-vertical spectral ratio) sites 1 to 16 (map sheet, Appendix A). Our analyses mostly yielded minimum depth to bedrock estimates, and to the extent that our measurements suggested possible bedrock response, it was for sedimentary rock, not basalt basement. The only exception is at site HVSR15. Several sites yielded resonant frequency (fr) values of about 0.2 (Appendix A), near the lower detection limit of our equipment and perhaps suggesting a response to sea waves, although somewhat higher fr values (higher-frequency sea waves) would likely prevail in our inland coastal setting (http://www.geopsy.org/documentation/geopsy/hv.html#idea). Because most of our estimates are minimum depths to bedrock, they do little to locate the western and southern boundaries of the Seattle basin. However, the -3,312 ft bedrock elevation estimate for HVSR4 (sec. 13, T25N R1W) next to the -2,526 ft estimate for HVSR5 (9,000 ft east of HVSR4) is inconsistent with an eastward-deepening of bedrock expected at the western margin of the Seattle basin. It may instead support the postulated presence of the Apex anticline and Anderson Creek syncline at the southern margin of the northwest-trending fault system shown on the map and along cross section A–A′–A″.

Structural observations, lineaments, aeromagnetic and gravity field strength orientations, selected bedrock depth estimates, seismic reflection data, and regional structural trends suggest to us that a dextral, northwest-trending strike-slip fault system traverses the map area and is locally expressed in right-stepping en echelon(?) faults with a surface pattern that suggests an underlying positive flower structure. We call this fault system the Dabob Bay fault zone (Fig. 1) because, even though the fault set we show extends farther east than Blakely and others' (2009) "DBF" (possible en echelon faults through Dabob Bay), Blakely (written commun., 2013) confirmed that the fault character, orientation, and geographic distribution that we propose match those envisioned by Blakely and others (2009). Our structural observations include faulted, distorted, disrupted, locally offset, and folded sediments at several sites that exhibit deformation expected within a northwest-trending, dextral transpression (or dextral wrench?) strike-slip fault system (Fig. 2) that likely extends southeastward into Bainbridge Island. We illustrate this apparent fault zone with several individual strands, some supported by observations of locally folded and/or sheared sediment, others only by geophysical data and well records analysis (see *Quaternary Structure and Neotectonics*, p. 7). Seismic profiles, aeromagnetic anomalies, and field exposures permit alternative interpretations and suggest that the fault zone is more complex and includes structures not shown on our map. We therefore query most fault strands and intend them mainly to illustrate the trends in the data we believe best explain the orientations of the structures in the map area.

Landscape Development

The map area is dominated by Pleistocene sediment. Bedrock is exposed only west of Hood Canal and includes Eocene marine sedimentary rocks (unit Em) north of Pulali Point (Squires and others, 1992) and basaltic and sedimentary rocks of the Eocene Crescent Formation (unit Ev_c) at and near Pulali and Wawa points (Tabor and Cady 1978; Yount and Gower, 1991).

PRE-VASHON SEDIMENT

On both sides of Hood Canal, we observed deposits derived from rock units found in the Olympic Mountains (Olympic-sourced) and delivered by pre-Vashon sedimentation into an otherwise ice-free Puget Lowland, most likely associated with ice advances in the Duckabush and Dosewallips basins west of the map area. These deposits typically contain clast assemblages of basalt, sandstone, and their common accessories and weathering products (chlorite, calcite, monocrystalline and polycrystalline quartz, and zeolites). Subsurface deposits in the Kitsap County portion of the Seabeck quadrangle are dominated by Olympic-sourced pebble gravel that we mapped as unit Qapo and interpret as braid-plain deposits from multiple pre-Vashon Olympic ice advances. We saw Olympic-sourced till among similar deposits (combined into unit Qad) only on the Toandos Peninsula and speculate that the recognition of till there and not elsewhere may be the result of superior exposure along the coastal cliffs of that peninsula and (or) that the till did not everywhere extend as far as the braid-plain deposits. We did not observe Olympic till on the Kitsap Peninsula, even where we had ample exposure (in and east of Big Beef Creek valley). Two possible exceptions are highly weathered till exposures at significant site S4 (sec. 22, T25N R1W) and paleomagnetic site N1 (sec. 12, T25N R1W). The lack of Olympic-sourced till on the Kitsap Peninsula suggests that Olympic ice advances did not extend much east of the Toandos Peninsula. Alternatively, the Olympic-sourced tills may be products of more proximal ice production in the Quilcene watershed. Elsewhere on the Toandos Peninsula, sediments lack till and include more sand, silt, clay, and peat. We interpreted these as nonglacial (unit Qc and subunits Qc_o and Qc_w).

On the Kitsap Peninsula, Olympic-sourced pebble gravel ceases to dominate the sedimentary section roughly at the boundary between the Seabeck and Poulsbo quadrangles. Deposits farther east and north increasingly incorporate northern-sourced glacial constituents deposited by or in response to southward advances of the Cordilleran ice sheet and nonglacial and proglacial constituents deposited by rivers from the Cascade Range (Cascade-sourced). In addition to sandstone and basalt, these sediments consist mostly of sand and silt derived from granitic and high-grade metamorphic rocks. They interfinger with unit Qapo. Peat and wood fragments, relatively rare in exposure but noted in a number of well records, suggest that in both the Seabeck and Poulsbo quadrangles, much of the silt, and to a lesser extent the sand, is nonglacial (unit Qc).

Exposures of moderately to well-sorted, gray to tan sand, and in some areas, silt, suggest uniform sand (or silt) packages at least a few tens of feet thick (units Qpos, Qpf, and Qgas). This sand is particularly prominent around Liberty Bay, east and west of Dyes Inlet, in the Anderson Creek basin, and at higher elevations in and near the Naval Base Kitsap at Bangor (NBK-B). The exposures generally lack organics, in places contain dropstones, and are marked by diverse clast compositions and dominantly south- to east-directed paleocurrent indicators. These attributes suggest a mostly Cordilleran-ice proglacial lacustrine setting for these units, with east-directed paleocurrents presumably documenting eastward deflection of outwash drainage around Green and Gold Mountains. Petrographic thin-section review of selected samples of unit Qpos revealed that some include a sand mineralogic mix equivalent to Snohomish River alluvium (Joe Dragovich, oral commun., 2013; Dragovich, 2007; Dragovich and others, 2007, 2010a,b, 2012). With the caveat that we have not excluded the possibility of similar mineralogy for deposits derived from some northern sources, we therefore suggest that some proglacial outwash may be older Cascade-sourced sediment reworked from the Puget Lowland. Some exposures mapped as proglacial outwash may also include nonglacial deposits. Unrecognized nonglacial deposits are also suggested by some well records that seem to report more organics than found in surface exposures.

Deposition of Cascade-sourced sand and silt at the western margin of the Puget Lowland during nonglacial times would imply a relative absence of coeval Olympic-sourced sedimentation. Such an absence is unlikely since the sedimentary section in most of the Seabeck quadrangle is dominated by Olympic-sourced braid-plain deposits (units Qapo and Qad). Voluminous Olympic Mountains sediment production is also recorded by extensive Olympic-sourced (proglacial) sedimentation on the west side of the Olympic Mountains during the Olympia nonglacial interval (MIS 3)(Fig. 3) and the Possession glaciation (MIS 4)(Thackray, 2001; Thackray and others, 2012; Glenn Thackray, Idaho State Univ., written and oral commun., 2012, 2013). Mineralogic similarity of the sand fraction in unit Qpos to Cascade-sourced alluvium might be explained by reworking of Cascade-sourced deposits

into drift associated with northern ice advances. The presence of similar mineralogic signatures in apparently nonglacial deposits on the Toandos Peninsula could be evidence that some nonglacial deposits are derived at least partly from this drift, or that the mineralogic signature is not unique to the source area of the present day Snohomish River. Alternatively, Contreras and others (2013) propose that Cascade-sourced sediment was directly transported into the map area during the Olympia nonglacial interval (MIS 3) by Cascade-sourced drainage and deposited into an elevated(?) lake setting. We therefore included some nonglacial deposits with sand mineralogy resembling Snohomish River alluvium as far west as the Toandos Peninsula in unit Qc$_O$, although their derivation may be debatable.

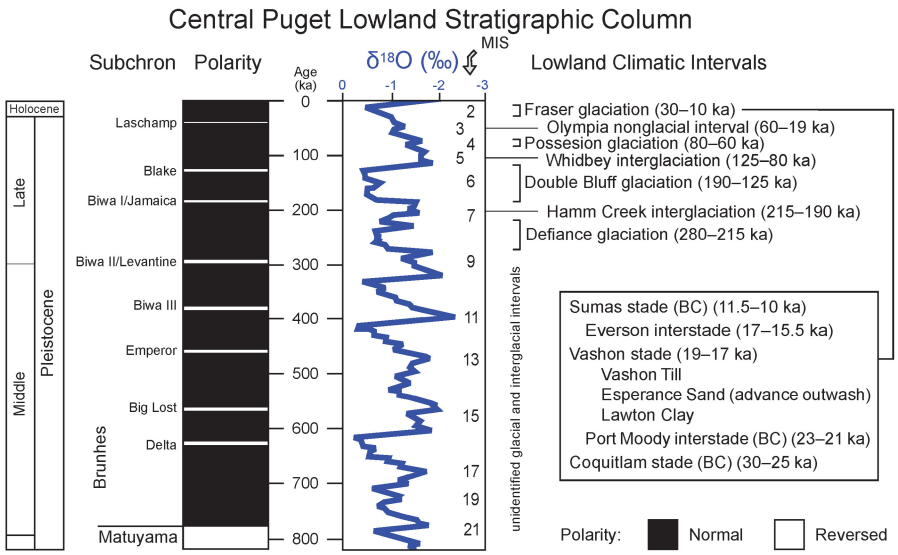

Figure 3. Comparison of geologic time scale, global magnetic polarity, marine oxygen isotope curve and stages (MIS), and ages of climatic intervals in the Puget and Fraser Lowlands [modified from fig. 6 of Troost and Booth, 2008]. Data sources are explained in Troost and Booth (2008). We modified age ranges for the Olympia nonglacial interval, Vashon stade, and Everson interstade to better conform with age control data from within the map area (GD7 and GD15, Tables B1, B2, B3) and near the map area (Beta 315794, Polenz and others, 2012c; QL-4067, QI-4065, and QL-4064, Anundsen and others, 1994, Porter and Swanson, 1998). We note that the exact time boundaries between the Olympia nonglacial interval, Vashon stade, and the Everson interstade in the Puget Lowland remain enigmatic.

Multiple pre-Vashon tills suggest that the oldest exposed sediment is of Defiance glaciation age (MIS 8)(Troost and others, 2003; Troost and Booth, 2008) or older. We observed three pre-Vashon tills (unit Qpt) in Big Beef Creek valley (map) and used well records to infer an additional, queried pre-Vashon till (unit Qpt) east of Big Beef Creek above 350 ft elevation (map and cross section A–A′). If this inference is correct, it implies pre-Defiance age for the oldest till (significant site S4, sec. 22, T25N R1W). Considerable weathering of that oldest till also supports relatively advanced age. Four pre-Vashon drifts are suggested by a composite section constructed from observations in the eastern Anderson Creek basin and along Hood Canal shoreline bluffs north of Anderson Creek (composite columnar section on map). The oldest till in that section, exposed a few feet above the beach along the Hood Canal shore (paleomagnetically normal site N1), is also very weathered. Review of well records and Anderson Creek–area field observations suggest three pre-Vashon tills in the Anderson Creek basin alone (cross section A′–A″). A widespread stratigraphic contact at about 200 to 250 ft between Anderson Creek and the east shore of Dyes Inlet separates Vashon from Possession outwash and appears to rise to 400 ft both toward the northeast and southwest. We have consequently mapped as pre-Vashon most of the outwash associated with Cordilleran ice. We favor the interpretation that tectonic activity at least partly explains a trough at Anderson Creek valley and exposure of several pre-Vashon drifts in the map area (*Quaternary Structure and Neotectonics*, p. 7, and cross section A–A′–A″). Alternatively, the gentle north-down slope from Green and Gold Mountains south of the map area to Hood Canal in the southern part of the Seabeck quadrangle may simply have produced plentiful pre-Vashon sediment exposures due to incision by relatively large drainages (Big Beef and Anderson Creeks).

To better constrain the age and character of the sediment in the map area, we obtained new paleomagnetic, pollen-based paleoenvironmental clast count and thin section petrographic, radiocarbon, and luminescence data. Specific inferences are noted in the relevant unit descriptions.

VASHON DRIFT

The modern landforms of fluted uplands and intervening troughs in the map area are largely a construct of the Fraser glaciation (MIS 2). Initial deposition of proglacial advance outwash in the “great lowland fill” was followed by

subglacial erosion and deposition of till (Booth, 1994). At the end of the glaciation, ice-dammed lakes and then marine waters filled the troughs (Bretz, 1910, 1913; Thorson, 1981, 1989; Dethier and others, 1995). As the ice dam(s) in the northern Puget Lowland wasted, lake levels dropped in stages, leaving behind a series of progressively lower and younger relict shorelines at discrete elevations (Haugerud, 2009; Ralph Haugerud, USGS, oral commun., 2013). Many of these relict shorelines are shown on our map, clustered at elevation ranges shown in Table 1. The shorelines are accompanied by relict drainage mouths and outwash channels, outwash terraces, alluvial fans, and deltas, some of which are mapped as unit Qgoaf. For example, at significant site S8 (sec. 25, T26N R1W), a relict shoreline is apparent north and south of a relict delta fan (unit Qgoaf) that is dissected by a modern drainage, which in turn terminates in a smaller, modern fan downslope. Association of relict shorelines with recessional glaciolacustrine conditions is best illustrated at date site GD15, where a quarry wall exposes lacustrine outwash sand (unit Qgos) in more than 20 rhythmites between two relict shorelines (see Fig. D2).

Table 1. Elevation ranges for clusters of relict shorelines noted within the map area (and shown on map).

	Relict shoreline elevation range (ft)																	
Likely associated relict lake	**Russell(?)**				**Russell**		**Bretz**								**Bretz or marine**			
Upper elevation within cluster of relict shorelines	500	420	400	380	310	275	220	200	180	130	120	100	80	35	40	30	10	
Lower elevation within cluster of relict shorelines	480	400	380	360	290	245	200	180	160	110	100	80	50	25	30	20	10	

Like Haugerud (2009) and Haugerud and Troost (2011), we relate shoreline elevation to specific water bodies and thus associate shorelines above 240 ft with Lake Russell (Bretz, 1910) and those below with Lake Bretz (Waitt and Thorson, 1983). We note that shorelines above 325 ft are unexpectedly high relative to the Lake Russell of Thorson (1981) but correspond to the combined clustering of Lake Russell shorelines and outwash channels graded to Lake Russell as identified by Haugerud (2009). However, our impression is that these shorelines, at least below 400 ft, correspond to lake or delta settings, not outwash channels (which could be significantly elevated above lakes). We do not know if the higher elevations of some shorelines resulted (partly?) from later land-level changes or from local lakes that may have been perched higher than Lake Russell. Our highest shorelines are near the southern map edge near the center of the map, conspicuously close to where cross section A–A′–A″ identifies pre-Vashon sediment at relatively high elevations, suggesting possible uplift of Pleistocene sediment.

Some shorelines below 40 ft are probably associated with glaciomarine inundation, at least in the northeast part of the map area, as also noted in the adjacent Suquamish quadrangle by Haugerud and Troost (2011), but we have been unable to separate those from lower Lake Bretz shorelines.

We note that shoreline elevation clusters occupy particular parts of the map area. For example, shorelines between 275 and 245 ft elevation tend to be found in a 2.5-mi-wide northwest-trending swath across the center of the Poulsbo quadrangle. Their locations overlap but are generally slightly southwest of those between 310 and 290 ft elevation. These distribution patterns are in part an expression of the extents of the lakes and of the isostatic rebound tilt documented by Thorson (1989), but we suspect that subtle tectonic signals also lurk among the distributions. For example, a shoreline between 360 and 340 ft elevation north of significant site S9 (sec. 17, T26N R1E) seems to be systematically 5 to 10 ft lower than the continuing(?) shoreline at 380 to 360 ft elevation to the south. Whether a similar offset is present in lower elevation shorelines to the west is unclear, in part due to apparent land surface modifications.

After draining of the glacial lakes and marine inundation, postglacial isostatic rebound raised the crust in the Puget Lowland, and local relative sea level dropped to below modern sea level (Dragovich and others, 1994; Mosher and Hewitt, 2004), causing valleys to incise to below modern sea level. This lower base level is recorded in many Puget Lowland drainages, where loose postglacial valley fill in the lower reaches extends below sea level. Such postglacial cut-and-fill to an elevation of at least -21 ft (below datum) is documented by subsurface sediment density contrast in a geotechnical report south of Stavis Bay, 35 ft south of the map boundary (Myers, 2011). We infer that since this early postglacial incision, geomorphic activity at the scale of the landscape has been minor—limited to coastal retreat, drainage extension (by headward erosion and deepening of upper valley reaches), and associated mass wasting.

Despite the relatively static condition of the modern environment, the distribution and character of sediments in the map area shows that geologic activity continues in the modern environment. This is illustrated along the shores

of Hood Canal by a transition from mostly steep coasts with narrow pebbly beaches or exposed bedrock along southern Hood Canal to broader shelves of sand or mud along northern Hood Canal. This steep coast–broad shelf transition seems to roughly coincide with the southwest edge of the Seattle basin as inferred near Holly by Contreras and others (2012b), suggesting that the structural transition from Seattle uplift to Seattle basin has controlled the distribution and character of past glacial and nonglacial deposition (and of modern exposure), which in turn has affected the type of sediment available for modern transport and nourishment of beaches.

Quaternary Structure and Neotectonics

SEATTLE FAULT

Many investigators have noted evidence for the west-trending Seattle Fault a few thousand feet south of the map area (Kimball, 1897; Raisz, 1945; Daneš and others, 1965; Gower and others, 1985; Bucknam and others, 1992; Haug, 1998; Blakely and others, 2002; Brocher and others, 2004; Kelsey and others, 2008; Tabor and others, 2011; Lamb and others, 2012). Lamb and others (2012) and Polenz and others (2012c) suggested that two south-up reverse faults and four folds associated with the Seattle Fault enter the map area beneath Hood Canal (southwest Seabeck quadrangle). Based on our review of supporting offshore seismic profiles, geomagnetic field strength, gravity and other previous work (Haug, 1998), we show these structures slightly modified from Lamb and others (2012). Like Lamb and others, we did not extend the structures eastward, where we were unable to satisfactorily interpret complex seismic profile data.

A new radiocarbon date from the east shore of northern Dyes Inlet (date site GD1) constrains the distribution of land level changes associated with activity on the Seattle Fault. A western redcedar stump and at least one other nearby stump are rooted in growth position in a relict peaty marsh mat that is overlain by more peat. Both peat layers are exposed in the modern intertidal zone and are being eroded by beach retreat (see Table B1; Fig. D1). We infer from the preservation of multiple stumps rooted in the lower woody peat mat that environmental change led to the death of the trees. A dense web of roots in the lower peat, in contrast to its absence in the upper peat, suggests that following tree death, environmental conditions inhibited resumption of tree growth, which is consistent with submergence after tree death. Abundance of mold spores, coupled with a lack of pollen and marine dinoflagellates in the upper peat, caused Estella Leopold (Univ. of Wash., written and oral commun., 2013) to comment that the upper peat resembles samples from brackish marsh settings elsewhere, consistent with estuarine inundation.

The stump yielded a radiocarbon date of AD 680–880 (Appendix B1). That age range does not overlap with the AD 900–930 timing inferred for the most recent earthquake on the Seattle Fault (Atwater, 1999), but we consider the two age estimates equivalent because the beach stump sample analyzed was an entire root segment with about 48 growth rings and bark (bark excluded from analysis), so that our sample included some older wood. The AD 680–880 age range may in any case underestimate true-age uncertainty (see Table B1).

Coincidence of tree death with a change in environmental conditions and the timing of a Seattle Fault earthquake and proximity to the Seattle Fault suggest that the stump may have died as a result of the Seattle Fault earthquake. The site provides evidence for absence of uplift and no clear evidence for or against subsidence in association with the Seattle Fault earthquake. We do not believe that the site experienced coseismic (sudden) uplift because that would not likely have led to death of the trees and preservation of the peat mat and stumps. Submergence after tree death could have resulted from gradual aseismic or coseismic subsidence, or from environmental change like breaching of a beach berm that protects a marsh from salt water influence (Brian Sherrod, written commun., 2012), and (or) a few feet of gradual sea level rise over the past 1,000 years (Eronen and others, 1987) to explain the present intertidal position of the relict peat. More detailed study (such as of plant assemblages and ages and diatom content at, above, and downsection of our stump) would therefore be needed to firmly link the tree deaths to the Seattle Fault earthquake and to determine whether or not the site underwent subsidence during or after the Seattle earthquake. The current record of our site extends westward the observation of Bucknam and others (1992) that the AD 900–930 Seattle Fault event did not trigger uplift at Winslow, about 8 mi east of our site and also a few miles north of the Seattle Fault. This contrasts with records of coseismic uplift at sites closer to the Seattle Fault (Kimball, 1897; Bucknam and others, 1992).

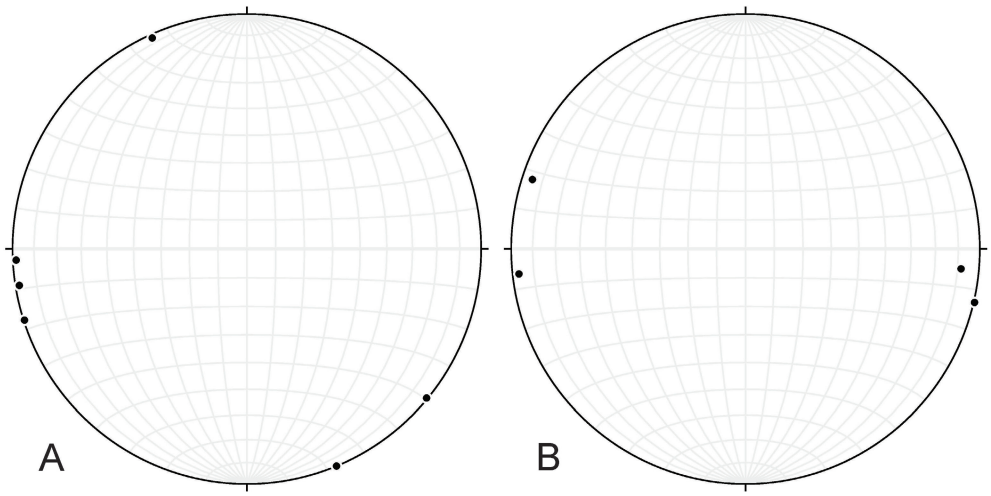

Figure 4. Equal angle stereonet plots of fold axes of deformed Pleistocene strata. **A.** Fold axes in rhythmically bedded silt along an eastern tributary of Anderson Creek at significant site S5 (sec. 13, T25N R1W; unit Qpf—due to map scale included with Qpos). Larger folds with axes trending north-northwest (on trend with the Anderson Creek syncline) define west-southwest-side-down monoclinal, outcrop-scale structures with amplitudes of several feet. Smaller folds with axes trending east appear as wrinkles with amplitudes of a few inches in otherwise planar bedding. **B.** Fold axes in interbedded silt, sand, and pebbly sand (unit Qc_O) along the east shore of Dyes Inlet south of Barker Creek at date site GD7 (sec. 21, T25N R1E)(*see* Fig. D4). Folds with axes that generally trend west to west-northwest define north- or north-northeast-side-down monoclinal structures with amplitudes of several feet. The post-depositional deformation and disruption by injection features resemble those along DBFZ fault 2 at paleomagnetic site N4 (sec. 20, T25N R1E), but the sum of exposures at N4 provides greater evidence of overall offset.

DABOB BAY FAULT ZONE

Broken, jumbled, faulted, and folded Pleistocene sediment, apparent fault offsets in seismic profiles, abundant northwest-trending magnetic anomalies, and geomagnetic suggestions of basalt bedrock depth variances all combine to suggest the northwest-trending, dextral strike-slip Dabob Bay fault zone (DBFZ)(see also *Tectonic Framework*, p. 1). We characterize this fault zone as dextral strike-slip based on regional context (the need to transfer strain from the west end of the Seattle Fault to the northwest or southwest, and orientation in common with the southern Whidbey Island fault zone) and our sense that observations throughout our map area fit this model. Evidence from specific parts of the map area is discussed below:

Total-field and upward-migrated geomagnetic field strength maps (Blakely, written commun., 2012, 2013) are marked by a northwest-trending fabric across the Poulsbo quadrangle. Topography does not explain this fabric, and we know no reason to suggest that bedrock depth or bedding orientations would. We infer that the fabric is most likely structural. If so, the pattern suggests a broad (>6 mi wide) northwest-trending zone of deformation that also extends southeast of the map area across Bainbridge Island north of the Seattle Fault. Geomagnetic anomalies within this northwest-trending fabric contributed to our placement of every DBFZ fault strand shown on the map but could similarly suggest many more. Those we drew are partly supported by additional data or are intended to illustrate our overall model without covering the whole map with speculative faults.

Most flutes and troughs in the map area trend south, ranging to south-southwest (210°) in the southern Seabeck quadrangle. A large number of topographic lineaments, subjectively noted at various scales, deviate from this orientation, trending in two clusters (315–330° and 335–350°) in broad alignment with the magnetic fabric. This trend is readily apparent in the mostly northwesterly alignment of drainages and modern shores in the Poulsbo quadrangle. We speculate that this pattern results from structural control. Additional clusters of lineaments trend 25–45° and 75–80°, suggesting a conjugate set of structures and more structural complexity than our general depiction of northwest-trending faults illustrates.

We infer DBFZ fault 1 beneath Dyes Inlet (southern Poulsbo quadrangle) based on seismic lines P 29 (a.k.a. line 27) and P29B (Dadisman and others, 1997). We obtained CDP (common depth point) shot point locations from Andrew Lamb (USGS, written commun., 2013) and locate the fault between CDPs 1061 and 1171, line P29B, and between 2201 and 2251, line P29 (line segment 1060 to 1690 ft south of map area, not shown). The fault offsets shallow sediment but does not clearly break the uppermost, postglacial sediment. An alignment of aeromagnetic

"max spots" (locations of anomalously large aeromagnetic field strength gradients, objectively identified by (computerized) curvature analysis, which assumes that contacts are vertical and remanent magnetization is unimportant)(Blakely, written commun., 2013) suggests a possible onshore extension to the northwest (not shown).

We infer DBFZ fault 2 based on a northwest-trending aeromagnetic anomaly and exposure of folded and broken sediment with sand injection features and shears (unit Qc, paleomagnetic sample site N4, sec. 20, T25N R1E) in a drainage west of Dyes Inlet. We observed that sediment exposures are offset across the drainage and some of its tributaries, and we observed an intervening disturbed zone marked by folded and broken sediment with sand injection features and shears, although it was not well exposed. We did not find a discrete fault plane that we could interpret as a definitive expression of a dominant northwest-trending fault. However, the orientations of features we measured are consistent with a northwest-trending fault across the area. Due to map scale, individual measurements are not shown. The minor northeast-plunging syncline shown at N4 is inferred from several measurements of bedding. No similarly disturbed sediment was observed in drainages to the north or south along the west shore of Dyes Inlet. We infer that the observed deformation is the likely result of a right-step from DBFZ fault 1 to DBFZ fault 2. We have no information about faulting of the upsection surficial deposits.

We infer both DBFZ faults 3 and 4 based on northwest-trending aeromagnetic anomalies and northeast-down offsets of Pleistocene sediment suggested by our analysis of well records.

DBFZ fault 5 on the Toandos Peninsula is exposed as a northwest-trending, right-lateral oblique reverse fault in sediment at significant site S2 (sec. 28, T26N R1W)(Fig. 5), where Carson (1975) previously noted a syncline as evidence for deformation on the Toandos Peninsula. The fault planes have an average orientation of N36°W, dipping 28°NE. The fault likely continues northwest along a northwest-trending aeromagnetic anomaly across Dabob Bay. We suspect that the anomaly and fault beneath Dabob Bay are associated with a slickensided contact exposed west of Dabob Bay between Crescent Formation basalt and overlying Eocene sedimentary rocks (unit Em).A radiocarbon date on gyttja at date site GD13 (sec. 28, T26N R1W) suggests that the faulted deposits are too old to date by radiocarbon. We tentatively assigned the faulted deposits to MIS 3 (unit Qc_o), but they could be older.

We infer DBFZ fault 6 based on northwest-trending aeromagnetic anomalies across the Kitsap and Toandos Peninsulas and on Hood Canal seismic profiles 76 and 93 (Dadisman and others, 1997; shot point locations courtesy Lamb, written commun., 2013) at shot point locations 2900 to 3300, line 76, and 1450 to 1650, line 93, coincident with a bend in that line. South-dipping bedrock reflectors south of the fault with on-lapping, flatter, upsection reflectors suggest a filled basin south of the fault. We infer that the fault extends northwest along aeromagnetic anomalies to significant site S1 (sec. 21, T26N R1W), where Carson (1975) noted a thrust fault exposed along Dabob Bay. The outcrop where Carson observed the fault was obscured by vegetation and colluvium when we visited the site.

Between DBFZ faults 6 and 7, seismic line 76 appears to record a broad zone of deformation. We suggest this portion of the fault zone is a positive flower structure that extends across the Toandos Peninsula. We extend DBFZ fault 7 across the Toandos Peninsula by relying on the north end of the deformed zone in the seismic lines and the broad trend of aeromagnetic anomalies, but we did not find field evidence to confirm the location of this fault.

Carson also suggested faulting on the east side of the Toandos Peninsula north of Hazel Point (sec. 27, T26N R1W). We observed the faulting he documented and infer that it is part of the wide zone of deformation along the Dabob Bay fault zone. We did not assign this exposure to a specific named strand. This location is depicted on the map as a minor fault striking N60°W and dipping 85°SW.

Buried organic matter in alluvial terraces in drainages near DBFZ faults 6 and 7 may be evidence of deformation near Dabob Bay. Radiocarbon date sites GD9 (sec. 16, T26N R1W) and GD12 (sec. 28, T26N R1W) suggest a change in base level during the past 2,000 years. A terrace at site GD9 may record uplift, while buried organic matter in a terrace at site GD12 suggest raising followed by lowering of base level. We caution that the mechanisms of terrace formation and abandonment are unresolved at both sites, and we were not able to link the age of the buried organic matter to known earthquakes or deformation. Old growth stumps on both terraces confirm prehistoric terrace formation, however.

Figure 5. Folded and faulted nonglacial deposits at Dabob Bay fault 5 (significant site S2; sec. 28, T26N R1W). Interbedded sand and pebble gravel (unit Qc_O) are folded and faulted along right-lateral-oblique reverse fault planes with an average strike of N36°W and dip of 28°NE. The beds have an estimated vertical offset of 20 ft across this fault. Carson (1975) reported a syncline at this location; however, the faulting was obscured by vegetation at that time. A view of the outcrop without the lines that trace individual fault planes in the image above is available in the archives of the Washington State Geological Survey blog at http://washingtonstategeology.wordpress.com/2012/11/09/november-geology-image-of-the-month-dabob-bay-outcrop/.

APEX ANTICLINE

Based on well records and field observations, we infer the north-northwest-trending Apex anticline southwest of the DBFZ as shown across the Kitsap Peninsula (map and cross section A′–A″). Sedimentary units at the west end of cross section A′–A″ rise gently northeastward before gently dropping farther northeast, consistent with a roughly 2-mi-wide northwest-trending anticline, the northeastern limb of which likely includes northeast-down, faulted offsets along DBFZ fault strands 3 and 4. Although the pattern is subtle and much of the well record data ambiguous, the anticline is also apparent in cross section G–G′ of Kahle (1998). This interpretation is reinforced by our observation of west-down folded lacustrine sediment in the valley walls of two eastern tributaries of Anderson Creek (significant site S5 [sec. 13, T25N R1W] and 200 ft east of date site GD5 [sec. 13, T25N R1W]) and a gentle west-down apparent dip on planar bedding in the drainage at date site GD2 (sec. 13, T25N R1W). A possible northwest extension (conservatively not shown on map) of the Apex anticline beneath Hood Canal is suggested by seismic reflectors south of DBFZ fault 6 (line 76, north of shot point 3701, 3,600 ft southwest of the fault), where reflectors suggest anticlinally deformed basin fill, consistent with (but narrower than) the anticlinal deformation we suggest in cross section A′–A″. We suspect the west limb of the Apex anticline may also be faulted but show no fault there because the inference is debatable and we lacked evidence for specific fault location(s).

ANDERSON CREEK SYNCLINE

The north-northwest-trending Anderson Creek syncline (map and cross section A–A′) is marked by coarsening-upward sections of lacustrine sediment. Dropstones and pebbly slurry facies, paucity of organic matter, and predominantly east- to south-directed paleocurrent indicators suggest that the lake deposits are mostly glacial. Intervening tills indicate that conditions conducive to lake sedimentation re-emerged over a span of multiple glaciations, suggesting possible Pleistocene basin growth. We observed west-down monoclinal folding in pre-Vashon lake sediments at significant site S5 (sec. 13, T25N R1W) and 200 ft east of date site GD5 (sec. 13, T25N R1W), and gently tilted sediment at date site GD2 (sec. 13, T25N R1W). West of Anderson Creek valley, the stratigraphic section is not conclusively correlated to that exposed in the basin but appears to be slightly elevated relative to the basin (cross section A–A′). Some tomographic images (figs. 6f, 6g, and 7 in Van Wagoner and others, 2002) suggest a possible bedrock depression at 2.5 and 20.5 km (1.6 and 12.7 mi) depth coincident with the inferred syncline, and seismic line data are consistent with the presence and westward broadening of the basin offshore to the north (line 91, shot point locations 1700 to 2800 in Dadisman and others, 1997). The syncline may be fault-bounded on both limbs.

OTHER OBSERVATIONS WITH POTENTIAL STRUCTURAL SIGNIFICANCE

At date site GD7 and paleomagnetic sample site N5 (secs. 20 and 27, T25N R1E) Olympia nonglacial–age (MIS 3) sand, mud, and pebble gravel exposed in and above the beach are folded (Fig. 4) and broken, and sand and mud facies are penetrated by injections of pebble gravel (*see* Fig. D4; Deeter, 1979). No obvious faulting was observed, except for minor shears, as visible in Fig. D4; however, a northwest-trending aeromagnetic anomaly (magnetic data courtesy Blakely, written commun., 2012, 2013) crosses the shore in a landslide complex at the south end of the exposure and suggests a fault parallel to the DBFZ fault strands we mapped beneath and west of Dyes Inlet.

At significant site S7 in an unnamed drainage west of Liberty Bay, a 15-ft-wide valley-floor exposure of compact, laminated, glaciolacustrine silt with dropstones appears to dip gently and uniformly north (strike 260°, dip 13° N). The origin of the dip is inconclusive, a landslide could not be excluded based on the exposure. From this site, an aeromagnetic anomaly trends 3 mi northwest to significant site S9 (and beyond into the Lofall quadrangle). A glaciolacustrine relict shoreline north of S9 appears to be 5 to 10 ft lower than to the south (based on use of lidar data for shoreline identification and elevation estimates).

At significant site S10 in another unnamed drainage west of Liberty Bay, stiff, compact, laminated clay (unit Qpf) in at least three different orientations is exposed across 20 ft of discontinuous section in the southern valley wall. The deformation could be due to mass wasting, tectonism, or glaciotectonism.

We infer the location of faults in Dabob Bay largely based on seismic lines (Dadisman and others, 1997) and aeromagnetic anomalies (Blakely, written commun., 2012, 2013).

Faulting at Tskutsko and Zelatched Points is suggested by exposures of older deposits (mapped as unit Qpd at Tskutsko Point) and Carson's report of deformed strata at Zelatched Point (significant site S3, sec. 32, T26N R1W; Carson, 1975). We mapped a queried fault at Tskutsko Point based on the older deposits and aeromagnetic anomalies but were less certain that the deformation at Zelatched Point is related to faulting.

DESCRIPTION OF MAP UNITS

We used USGS Fact Sheet 2010-3059 as time scale (USGS Geologic Names Committee, 2010) and the Udden-Wentworth scale (table 5 in Pettijohn, 1957) to classify unconsolidated sediment. We identified units from field work, geomorphic expression (including lidar—Puget Sound Lidar Consortium, 2000, http://pugetsoundlidar.ess.washington.edu/), field relations, sediment thin sections, well records, geophysical data, prior mapping (including nongeologic mapping with geologic implications, such as "T-sheet" historical topographic surveys along coastlines—http://riverhistory.ess. washington.edu/data.php), and aerial orthophotos (2009 30-cm color; 2007 12-in. color; 2011, 2009, and 2006 1-m color; 2011 3-ft infrared; 2003–2005 18-in. color; 1990–2000 3-ft black and white). We used LANDSAT satellite image analysis calibrated against our own field observations to develop gridded satellite images that reveal trends in surface sediment particle size to supplement our observations. For radiocarbon dates that lacked age statements in calendar years but were not too old for calibration, we used OxCal online, v. 4.2 (sample UW 446, accessed April 11, 2013, and sample Ql 4064, accessed April 12, 2013, at http://c14.arch.ox.ac.uk/embed.php?File=oxcal.html), to convert from the reported "radiocarbon years" (^{14}C yr BP, expressed to 1σ) to calendar years before 1950 (cal yr BP, or ka, expressed to 2σ; Bronk Ramsey, 2009); these conversions rely on the

IntCal 09 calibration curve. To map Naval Base Kitsap at Bangor, we referred to two guided base tours (without sampling opportunities), prior geologic and geomorphic mapping (Kahle, 1998; Birdseye, 1976; consultants' reports; McKenna and others, 2008; Haugerud, 2009), the national wetland inventory (http://www.fws.gov/wetlands/ and U.S. Fish and Wildlife Service, written commun., 2013), well records (Kahle, 1998; Wendy Welch, USGS, written commun., 2012; Paterson, 1981; Kitsap Public Utility District, written commun., 2012; well logs from WADOE), lidar, aerial photos, and surface sediment particle size information from LANDSAT satellite data.

Quaternary Unconsolidated Deposits

HOLOCENE NONGLACIAL DEPOSITS

af **Artificial fill**—Sand, cobbles, pebbles, boulders, silt, clay, organic matter, rip-rap, and concrete placed to elevate the land; engineered or non-engineered; shown where readily verifiable, fairly extensive, and apparently thick enough (>5 ft) to be geotechnically significant; excludes roads, most fills within the NBK-B, and areas where underlying geology was deemed more informative. There is a map edge mismatch with the Suquamish quadrangle south of Keyport (sec. 36, T26N R1E) where we identified fill that Haugerud and Troost (2011) included in a larger modified land area.

ml **Modified land**—Locally derived sand, pebbles, cobbles, boulders, silt, clay, or diamicton excavated and redistributed to modify topography; underlying units exposed in some cuts; locally includes concrete and artificial fill; shown where fairly extensive and apparently thick enough (>5 ft) to be geotechnically significant; excludes roads, inactive pits where underlying units can be identified, modifications within the NBK-B, and areas where underlying geology was deemed more significant.

Qb **Beach deposits**—Sand, pebbles, pebbly sand, cobbles, silt, clay, shells, wood, peat, and isolated boulders; loose; clasts typically moderately to well rounded and oblate; locally well sorted; derived from shore bluffs, streams, and underlying deposits. Unit Qb is transient in the modern environment; erosion at times exposes underlying units. The age of unit Qb is constrained to less than about 6,000 years because before that time, sea level was much lower (Dragovich and others, 1994; Mosher and Hewitt, 2004).

Qa_m **Marine deltaic alluvium**—Sand, mud, and in channel bedload facies, pebbles, and cobbles; includes some organic salt-marsh deposits; clasts and matrix generally fresh; loose; clasts typically well rounded; moderately to well sorted; stratified to massively bedded; deposited in tide flats and stream channels below high-tide level; distinguished from unit Qa by presence of brackish water. Like unit Qb, the age of unit Qa_m is constrained to less than about 6,000 yr. There is a boundary mismatch with the Wildcat Lake quadrangle (Tabor and others, 2011) south of Stavis Bay (sec. 25, T25N R2W) where the map edge approximates a transition from salt marsh (Seabeck quadrangle) to freshwater alluvium (Wildcat Lake quadrangle).

Qm **Marsh deposits**—Organic sediment and (or) loose clay, silt, and sand in tidal flats and coastal wetlands; saltwater to brackish equivalent of unit Qp (described below). There is a map edge mismatch with the Suquamish quadrangle (Haugerud and Troost, 2011) south of Keyport (sec. 36, T26N R1E) where we, unlike Haugerud and Troost, distinguished between intertidal marsh and valley floor alluvium.

LATEST PLEISTOCENE TO HOLOCENE NONGLACIAL DEPOSITS

USGS Fact Sheet 2010-3059 puts the age of the Holocene–Pleistocene boundary at "11,700 ±99 yr". Luminescence data from GD15 (sec. 25, T25N R1W) suggest partial Vashon ice collapse and formation of Lake Russell at about 17 ka (Tables B2 and B3). Radiocarbon data suggest post-Vashon ice-free conditions by about 16 ka at Lake Carpenter (Anundsen and others, 1994; Porter and Swanson, 1998), 6.2 mi northeast of the map area, and that glaciomarine inundation had ceased by about 14 ka (Anundsen and others, 1994, sample QL-4064, 12,450 ±140 ^{14}C yr BP; OxCal online conversion to calendar years yielded a 2σ age estimate of 15,104–14,049 cal yr BP, thus supporting an end of glaciomarine inundation by about 14 ka). We therefore distinguish between Holocene units and units that range from Pleistocene to Holocene age.

Qp **Peat**—Organic and organic-rich sediment; includes peat, gyttja, muck, silt, and clay; typically in closed depressions; commonly mapped on the basis of topography or aerial photos; mapped in all recognized wetland areas and flat-bottomed closed depressions unless a different unit or standing water was identified.

Qls **Landslide deposits**—Cobbles, pebbles, sand, silt, clay, boulders, or diamicton in landslide bodies and toes; clasts and grains angular to rounded; unsorted; generally loose, jumbled, and unstratified, but locally retains primary bedding and compaction; commonly includes liquefaction features. Absence of a mapped slide does not imply absence of sliding or hazard. Many slide areas are unmapped because they proved too small to show, or steep slopes, beach waves, or streams have dispersed their deposits. Slides not recognized with confidence are shown as unit Qmw. Some slide areas include exposures of underlying units. Where map scale permits, head scarps are identified by a scarp symbol. There is a map edge mismatch with the Wildcat Lake quadrangle (Tabor and others, 2011) east of Big Beef Creek (sec. 27, T25N R1W) where Tabor and others included a landslide-affected slope with Vashon advance deposits and with the Suquamish quadrangle east of Crouch Creek (sec. 13, T25N R1E) where Haugerud and Troost (2011) terminated a landslide polygon upslope of a road that we included in the landslide polygon.

Qmw **Mass-wasting deposits**—Cobbles, pebbles, sand, silt, clay, boulders, or diamicton; typically loose; generally unsorted; locally stratified; mapped along mostly colluvium-covered or densely vegetated slopes that are potentially or demonstrably unstable; locally includes alluvial fans, debris fans, landslides too small to show separately or that could not be confidently mapped, and exposures of underlying units. At significant site S3 (sec. 32, T26N R1W), we mapped mass wasting deposits based on signs of instability in the bluff but were not convinced that the deformation is entirely related to mass wasting. Carson (1975) observed faulting of sediment in the bluff and concluded that the deformation was tectonic. Absence of a mapped mass-wasting deposit does not imply absence of slope instability or hazard.

Qa, Qoa **Alluvium**—Pebbles and sand, locally cobbles, silt, clay, and peat; clasts and matrix generally gray and fresh, but some exposures iron-stained; loose; clasts typically well rounded and moderately to well sorted; stratified to massively bedded; deposited in streams and on flood plains and terraces. The unit may locally include recessional outwash (unit Qgo). Subunit Qoa resembles unit Qa but is older and forms elevated relict terraces that (unlike terraces mapped as unit Qgo) lack evidence to link them to a recessional glacial environment; however, unit Qoa likely includes some recessional glacial deposits. The relict character of unit Qoa is documented by identification of Mazama tephra (probable age 6,730 ±40 ^{14}C yr BP, Franklin Foit, Wash. State Univ., written commun., 2012; Zdanowicz and others, 1999; Hallett and others, 1997) at geochemical sample site G1 (sec. 8, T25N R1E; Table C1). Radiocarbon dates of 1,349 ±32 yr BP and 2,010 ±30 yr BP at sites GD9 and GD12 (secs. 16 and 28, T26N R1W; Table A1) on the western Toandos Peninsula also suggest that relict terraces in an unnamed stream and along the shore may be related to tectonic movement—or simply a sediment pulse. However, although the region is tectonically active (see *Quaternary Structure and Neotectonics*, p. 7), we have not locally identified a tectonic mechanism or other evidence for tectonically induced terrace abandonment and preservation. Along stream reaches graded to modern sea level, units Qa and Qoa should be younger than about 6,000 years (see also unit Qb, p. 12). Sand, silt, or peat facies locally dominate gently sloping areas, such as in secs. 7 and 18, T25N R1E (Poulsbo quadrangle, south of NBK-B). Post-glacial alluvium is unit Qoa where relict. Unit Qoa includes a relict alluvial fan along big Beef Creek. There is a map edge mismatch with the Wildcat Lake quadrangle at Big Beef Creek (sec. 27, T25N R1W) where Tabor and others (2011) included alluvium with Vashon advance deposits.

Qaf, Qoaf **Alluvial fan deposits**—Pebbles, sand, cobbles, boulders, and silt; loose; moderately to poorly sorted; stratified to poorly stratified; forms concentric lobes where streams emerge from confining valleys. Deposition is commonly sudden, hazardous, and associated with significant storm events, such as the storm of December 1 to 3, 2007 (Sarikhan and others, 2008). Relict fan deposits that have stopped accumulating because modern streams are sufficiently incised to pre-empt addition of modern sediment are identified as unit Qoaf near the northwestern map corner. We speculate, but lack strong evidence, that

these fans may be glaciorecessional and graded to a lower stage of Lake Bretz or the glaciomarine sea level maximum, which likely approximated or slightly exceeded modern sea level in this part of the Puget Lowland. The glaciorecessional relationship is suggested by apparent glaciomarine shorelines and deposits at Liberty Bay (this study; Haugerud and Troost, 2011) and a record of multiple episodes of glaciomarine inundation a few miles northeast of the map area at Carpenter Lake (secs. 26 and 27, T27N R2E; Anundsen and others, 1994). Unit Qgoaf (described below) is distinguished from unit Qoaf by field relations that more strongly suggest or require deposition of unit Qgoaf coeval with Vashon recessional outwash. There is a map edge mismatch with the Wildcat Lake quadrangle west of Big Beef Creek (sec. 27, T25N R1W) where Tabor and others (2011) included a surficial alluvial fan with Vashon advance deposits.

PLEISTOCENE GLACIAL AND NONGLACIAL DEPOSITS

Exposures of the stratigraphically highest drift were systematically assigned to the Vashon stade of the Fraser glaciation (MIS 2) unless we had specific reason to map an older drift. Where we lacked specific reason to assign a pre-Vashon deposit to a specific drift or nonglacial unit, we assigned pre-Vashon deposits to undifferentiated units—Qpd, Qpt, Qpog, Qpos, and Qpf for continental glacial deposits originating from the north, Qapo for alpine glacial deposits originating from the Olympic Mountains, Qc for nonglacial deposits, and Qpu for deposits of unresolved association.

We used clast counts, petrographic review of sand content, sedimentary attributes (such as paleocurrent indicators and upward-coarsening of sections), and field relations (such as that Hood Canal prevents post-Vashon transport of sediment from the Olympic Mountains into the map area) to determine sedimentary sources and infer the source area of glacial ice. Clast compositions in nearly all deposits in the map area are dominated by sandstone and (or) basalt. Sedimentary clasts included primarily medium to dark gray or brown and commonly micaceous sandstone, with lesser mudstone and conglomerate.

Based on clast composition in samples of modern alluvium and Vashon glaciorecessional outwash from the lower Dosewallips and Quilcene Rivers, we assumed sediment consisting of almost exclusively sedimentary rocks and mafic volcanic rocks (basalt) to originate primarily from the Olympic Mountains (see also Qapo, p. 18), although many samples likely include other proximal bedrock sources, such as the Port Ludlow area north of the map area and Green and Gold Mountains south of the map area. Sandstone and basalt have also been transported into the map area from more distal sources (Coast Mountains of British Columbia, Cascade Range of Washington, San Juan Islands). Olympic-sourced deposits dominate units Qapo and Qad, in which we rarely estimated more than 4 percent diagnostically northern-sourced clast content (including plutonic and high-grade metamorphic rocks).

Plutonic rocks containing quartz and (or) potassium feldspar (granite) and rocks containing primarily plagioclase feldspar (diorite or gabbro) and diverse assemblages of other rock types (notably high-grade metamorphic rocks) were assumed to indicate sediment from northern-sourced (Cordilleran ice sheet) glacial advances from the Coast Mountains of British Columbia. Some clasts that we field identified as “dioritic” or “gabbroic” could include leucogabbro from bedrock at Green Mountain to the south in the nearby Wildcat Lake quadrangle (Tabor and others, 2011), and detritus from granitic rocks could also have reached the map area from the Cascades east of the map area, as was suggested by Dragovich (Wash. Div. of Geology and Earth Resources [DGER], oral commun., 2013) based on his petrographic review of selected sand fraction samples from our map area. We generally estimated 10 to 32 percent diagnostically northern-sourced clast content in deposits that we mapped as northern-sourced, although estimates ranged to 50 percent. We estimated sandstone content (includes siltstone and lightly metamorphosed rocks consistent with Olympic-core sources) between 17 and 60 percent, and basaltic rock content between 19 and 58 percent (with poorly constrained maximum estimates of 73 and 75%).

Vashon Drift

Vashon advance outwash and till are bracketed in the map area by a 16,510 ±320 ^{14}C yr BP date on wood from below Vashon Drift at date site GD7 (sec. 21, T25N R1E)(*see* Fig. D4; Deeter, 1979, UW 446, OxCal 2σ age range 20.360–18.922 ka). A new 17.130 ±1.080 ka luminescence age estimate (1σ; Tables B2 and B3) on sand from GD15 (sec. 25, T25N R1W; Fig. D2) dates partial Puget lobe ice disintegration and formation of Lake Russell (or, less likely, a more local lake at similar elevation). Additional radiocarbon data from west and southwest of the map area suggest that Vashon ice may have advanced later than 18.9 ka (Polenz and others, 2010, 2011, 2012a,b,c). Radiocarbon dates from northeast of the map area suggest post-Vashon, ice-free conditions by 16 ka (see *Latest*

Pleistocene to Holocene Nonglacial Deposits, p. 12; Anundsen and others, 1994; Porter and Swanson, 1998). The sum of these dates suggests that Vashon ice entered the map area later than envisioned by Porter and Swanson (1998) and Booth and others (2004), then stalled at its southern terminus and quickly disintegrated (Logan and Walsh, 2009; Haugerud, 2009; Polenz and others, 2012b,c), although patches may have persisted for millennia (Porter and Carson, 1971).

Qgo **Vashon recessional outwash**—Sand and pebble and cobble gravel, some silt and clay; clasts and matrix mostly fresh, but commonly iron-stained to brown, red, and yellow, and in some exposures more weathered than recent alluvium; clasts subrounded to well rounded; moderately sorted and stratified. Pebbly facies of this unit are common in outwash channels, and loose, sandy pebble gravel with rounded clasts was mapped as part of the unit in a set of outwash channels along the southern map edge of the Poulsbo quadrangle NW¼SW¼ sec. 25, T25N R1W. That deposit may be subglacial, based on channel morphology with relatively rounded channel edges (and by likely ice proximity suggested by dominance of angular matrix silt and clay particles, as detected by feel of hand sample). Also included in the unit is a set of terraces below 40 ft elevation along the south shore of Liberty Bay. These surfaces are cored by brown mud that we interpret as glaciomarine tideflat deposits. We similarly interpret a fan at the northwest end of Dyes Inlet as glaciolacustrine (or glaciomarine?) and fans and surfaces between 100 and 180 ft elevation in Bangor as glaciolacustrine. We interpret a luminescence date on rhythmically bedded sand from GD15 (sec. 25, T25N R1W; Tables B2 and B3) as early Lake Russell–age and infer that recessional outwash deposition (unit Qgo and subunits) may have begun by 17 ka (see *Vashon Drift*, p. 5). We prefer the IRSL analysis on feldspar (17.130 ±1.080 ka, 1σ; Tables B2 and B3) to the OSL analysis on quartz (Tables B2 and B3) because the quartz analysis proved challenging, as is typical in Washington (Shannon Mahan, USGS, oral commun., 2013). There are map edge mismatches with the Wildcat Lake quadrangle south of Stavis Bay (sec. 25, T25N R2W) and west of Seabeck Creek (sec. 29, T25N R1W), where Tabor and others (2011) included recessional outwash with adjacent advance outwash along the same slope. Subdivided into:

Qgoaf **Vashon recessional alluvial and delta fan deposits**—Pebble gravel, sand, silt, and boulders; loose; moderately to poorly sorted and stratified; form concentric lobes where streams once emerged from valleys; mapped in the Poulsbo quadrangle west of Liberty Bay and Dyes Inlet, east of Hood Canal on NBK-B (sec 19, T26N R1E), and in sec. 24, T25N R1W (4,000 ft north of date site GD15 near the southwest quadrangle corner). Most deposits of unit Qgoaf are associated with relict shores and are thought to be deltaic, such as east of significant site S7 (sec 27, T26N R1E). We speculate that a set of relict fans at the northwest corner of the Seabeck quadrangle may also be glaciorecessional but, like Polenz and others, 2012c, mapped these fans as unit Qoaf because we did not recognize an associated shoreline and were less confident of glaciomarine or glaciolacustrine association.

Qgos **Vashon recessional outwash sand**—Sand and some beds and lenses of pebbles, silt, and clay; gray to tan; clasts moderately to well rounded; moderately to well sorted and stratified; loose and generally less compact than glacially overridden outwash sand (units Qgas and Qpos). Most deposits are slackwater deposits into a recessional lake setting, such as at date site GD15 in the southwest corner of the Poulsbo quadrangle (sec. 25, T25N R1W; Fig. D2).

Qgof **Vashon recessional glacial lake deposits**—Silt, sand, clay, and rare dropstones; gray; loose, locally moderately stiff; moderately to well sorted; laminated or massive. The greatest unit thickness we know of is in the southeast corner of the Poulsbo quadrangle at site HVSR 7 (sec. 14, T25N R1E), where our analysis of seismic measurements suggests 40 ft.

Qgic **Vashon ice-contact deposits—**Cobble and pebble gravel, sand, lacustrine mud, and isolated boulders, with discontinuous deposits of ablation, flow, and lodgment till; commonly light (or ash) gray, ranging to tan or brown; loose to compact; poorly to well sorted; massive to well stratified. Unit Qgic locally includes oversteepened beds that developed (1) due to sub-ice flow dynamics, (2) as collapse features following melting of nearby ice, or (3) by glacio(?)-tectonic deformation. Unit thickness ranges from a

few feet to more than 100 ft as shown in the southwest corner of the Seabeck quadrangle and in cross section A–A′. Unit Qgic was primarily deposited late in the glaciation by meltwater and ice. The unit typically coincides with ice-contact features that we tend to associate with stagnant ice, such as ripples on flutes, disrupted surfaces on and between flutes, kettles, hummocky topography, subglacial or subaerial outwash channels, and eskers (also separately mapped as unit Qge at northwest map corner). Where morphologic evidence for stagnant ice is weak or absent, unit Qgic is mapped from observation of absence or poor development of till matrix, with such till typically containing less mud and being more friable than well-developed lodgment till (unit Qgt). Where stagnant-ice features are found (and mapped as unit Qgic), lodgment till is commonly absent or only a few feet thick, locally ranges to "sub-glacially reworked till" (Laprade, 2003), and tends to be more permeable and less compact than well-developed lodgment till. See also Polenz and others (2009a,b, 2010a, 2011), Contreras and others (2012b), and Haugerud (2009) for discussion of the Fraser glaciation, leaky till, and similarities among units Qgic and Qgo and subunits Qgos, Qgof, and Qgol east and south of the map area. Some boundaries to unit Qgo are gradational. There are map edge mismatches with the Wildcat Lake quadrangle (Tabor and others, 2011) west and east of Seabeck and Big Beef Creeks (secs. 25–30, T25N R1W) where we in places mapped weakly developed lodgment till as unit Qgic, whereas Tabor and others made no distinction between that and well-developed lodgment till. East of Seabeck Creek (sec. 29, T25N R1W), Tabor and others also mapped Vashon advance outwash where we identified unit Qgic. Locally divided into:

Qge **Vashon esker—**Pebble to cobble gravel and sand; tan to brown; loose; clasts moderately to well rounded; typically well sorted; predominantly basaltic clasts; forms low, elongate, sinuous hills; mapped in areas thought to be occupied by stagnant ice in the northwest portion of the map.

Qgt **Vashon lodgment till**—Diamicton, mostly lodgment till, consisting of clay, silt, sand, pebbles, cobbles, and isolated boulders, typically supported by a hard, muddy, sandy matrix; brown to gray, ranging to tan; typically lightly weathered or unweathered; compact, with well-developed facies resembling concrete, but near the surface commonly hackly or looser and with loose ablation till composing the top 1 to 10 ft; clasts commonly striated and faceted, with subangular or rounded edges; unsorted; unstratified (but locally banded); forms a patchy and seemingly randomly distributed cover, with typical exposures 3 to 15 ft thick. We generally estimated diagnostically northern-sourced clast content (including plutonic and high-grade metamorphic rocks) between 10% and 22%, sandstone content between 23% and 60%, and basaltic content between 19% and 58% (estimates ranged to 75%). The thickest clearly observed exposure is in a gravel pit in the southwest corner of the Poulsbo quadrangle at significant site S6 (sec. 19, T25N R1E), where till unit thickness steadily increases from 5 to 30 ft in the eastern pit wall to 80 ft thick 1,100 ft farther west. Unit Qgt was deposited directly by glacial ice. Plutonic, basaltic, and metamorphic erratic boulders up to 6 ft in diameter are common in and on till. Some exposures include locally sheared and jointed lenses or layers of sand, pebbles, and cobbles. Unit Qgt typically dominates, but is discontinuous on, fluted surfaces. Well-developed lodgment till locally forms an effective aquitard, but varied till thickness and gradational association with more permeable ice-contact deposits and outwash channels suggest that the aquitard is leaky (Polenz and others, 2009a, 2010a; Contreras and others, 2012b; Haugerud, 2009).

We mapped unit Qgt where we observed stronger lodgment till development—and typically also better development of fluting. We associate unit Qgic with presence of other ice-contact deposits and lesser lodgment till development. Unit Qgt is typically in sharp, unconformable contact with underlying units. Unit Qgt lies stratigraphically below unit Qgo. Unit Qgt may include surficial exposures of Olympic-sourced till (unit Qad) or older till, as suggested in cross section A′–A″ west of State Route 3, where well records suggest that older subsurface till meets Vashon till at the surface. Vashon till in the map area displayed greater differences in clast lithology from site to site than principal investigator Michael Polenz has noted in any Puget Lowland mapping project during more than 10 years of mapping. We suspect this diversity represents reworking of diverse Puget Lowland subsurface deposits and more distal deposits, and we suggest that lodgment till composition in the map area is dominated by proximal (Puget Lowland subsurface) sources. There are map edge mismatches with the Suquamish quadrangle (Haugerud and Troost, 2011) north of Keyport (sec. 25, T26N R1E) where we chose to identify the

Everson marine incursion by reference to a relict shoreline at 30 to 40 ft elevation and Haugerud and Troost mapped a thin and spotty cover of Everson emergence gravel (relict glaciomarine beach sediment—Domack, 1983). Additional mismatches resulted farther north (secs. 13, 24, and 25) where Haugerud and Troost mapped Vashon advance outwash sand.

Qga **Vashon advance outwash**—Pebble and cobble gravel, sand, silt, and clay; low mud content in matrix except in ice-proximal and glaciolacustrine deposits that can locally include diamicton, most likely from debris-flow deposits; gray to tan; generally compact (see fig. 4 of Polenz and others, 2009a), but commonly cohesionless; clasts typically well rounded and well sorted; very thinly to very thickly bedded, with planar and graded beds, cut-and-fill structures, trough-and-ripple crossbeds, and foresets, but ranges to structureless. At the southwestern map corner, unit thickness appears to exceed 200 ft, based on western valley-wall exposure and similar observations by Polenz and others (2012c) west of the map area. A 130-ft-high and more than 1,000-ft-wide pit wall exposure at significant site S6 (sec. 19, T25N R1E, mapped as unit ml because mining continues) forms a generally coarsening-upward section of sand and pebble gravel, consistent with Booth's (1994) model of a regional lowland fill. We mapped the unit down to sea level only at the southeast and southwest ends of the map area. At the southwest end, age control is lacking, but so are indications of pre-Vashon age. The deposits between Stavis Bay and Seabeck Creek appear to drape older units locally exposed upslope. At the southeast end of the map area, subunits Qgas and Qgaf are extensively mapped because a 16,510 ±320 ^{14}C yr BP date on wood at date site GD7 (sec. 21, T25N R1E; Deeter, 1979, UW 446, OxCal 2σ age range 20.360–18.922 ka), if correct, demands a late Olympia-age (MIS 3) for apparently underlying deposits. Elsewhere throughout the map area, we inferred that similar deposits near sea level are of pre-Vashon age, based on well records and apparently or demonstrably upsection exposures of older drifts and of sediment from Olympic sources. We similarly inferred that the base of the unit rises above 400 ft across the center of the map area (cross section A–A′–A″). We attribute this to paleotopography but note that at least some of that topography appears to have developed due to Pleistocene uplift along the Apex anticline, and perhaps also west of Anderson Creek. The similarly elevated bottom for the unit at the north end of the Poulsbo quadrangle is based partly on Contreras and others' (2013) interpretation that Olympia-age (MIS 3) deposits are present at an elevation of 400 ft at the northern map boundary. Unit Qga is from northern sources and was deposited as proglacial fluvial, deltaic, and lacustrine sediment during the Vashon glacial advance. It is typically overlain by units Qgt or Qgic along a sharp, unconformable contact. There is a map edge mismatch with the Wildcat Lake quadrangle (Tabor and others, 2011) at the southwestern map corner and west of Seabeck Creek, where Tabor and others included valley walls with valley floor alluvium (southwest map corner) or Vashon till (west of Seabeck Creek, sec. 29, T25N R1W), whereas we identified older units midslope. Subdivided into:

Qgas **Vashon advance outwash sand—**Sand, in some exposures pebbly or with interbeds of silt, clay, pebbles, cobbles, or diamicton; matrix mud content generally low; gray to brown; generally compact; particles typically subrounded or well rounded and moderately to well sorted; very thinly to very thickly bedded; contains planar and graded beds, cut-and-fill structures, trough-and-ripple crossbeds, and foresets, but also locally structureless. Unit Qgas was mapped extensively only near southeastern map corner. Based on field relations and well data interpretations, we mapped otherwise similar deposits at similar elevations elsewhere in the map area as pre-Vashon.

Qgaf **Vashon advance lacustrine mud—**Glaciolacustrine silt, locally appears to range to clay, locally with dropstones or interbeds of sand, pebbles, cobbles, or diamicton; gray to brown; compact; typically well sorted; laminated to massive; maximum observed thickness about 80 ft southwest of Burke Bay (secs. 14 and 23, T25N R1E). Unit Qgaf was extensively mapped only near southeastern map corner. Based on field relations and well data interpretations, we mapped otherwise similar deposits at similar elevations elsewhere in the map area as pre-Vashon.

Pre-Vashon Glacial Deposits

Pre-Vashon Olympic-Sourced Glacial Deposits

Qad **Pre-Vashon alpine drift**—Diamicton (till) and outwash composed of Olympic-sourced basalt and minor sandstone clasts; gray to red-brown; loose to very compact; clasts typically subangular to subrounded; moderately sorted to unsorted and unstratified; outwash generally horizontally bedded or crossbedded. Unit Qad includes alpine till, diamicton, and outwash deposits on the Toandos Peninsula. Unit Qad appears to have been deposited as pulse of alpine drift into an otherwise nonglacial Puget Lowland, and assuming that a downsection 35,210 ±320 ^{14}C yr BP date (date site GD14, sec. 4, T25N R1W) is valid, was deposited late during the Olympia nonglacial interval (MIS 3) or early in the Fraser glaciation (MIS 2).

Qapo **Pre-Vashon alpine outwash**—Pebble to cobble gravel with sandy to clayey matrix, locally bordering on diamicton, with interbeds of sand, silt, and clay, sparsely exposed organic-rich mud, peat, and woody detritus, and rare bouldery cobble gravel facies; light reddish-brown to dark brown, typically darker and more reddish than northern-sourced outwash, less commonly gray; variously weathered, ranging from fresh to mostly saprolitized clasts; compact; clasts mostly subrounded; moderately sorted; generally level-bedded with widespread, gentle crossbeds, but ranging to structureless. We estimated sandstone clast content (including siltstone and lightly metamorphosed rocks consistent with Olympic-core sources) in unit Qapo from 39–78%, basalt content from 8–48%, all other rocks in most samples comprise less than 10%.

Although cross section A–A′ suggests more than 600 ft of Qapo unit thickness in part of the Seabeck quadrangle, this section is very likely interrupted by northern-sourced till(s), and the maximum uninterrupted unit thickness is unclear. We interpret unit Qapo as an Olympic-sourced, alpine proglacial braid-plain deposit, mostly from an ancestral Dosewallips River, into an otherwise nonglacial Puget Lowland setting. We base that assessment on (1) dominantly east- to north-directed paleocurrent indicators; (2) dominance of pebble to cobble gravel that we interpret as indicative of higher sedimentation rates compared to the modern nonglacial Puget Lowland, although the gravel includes interbeds, typically between 2 and 10 ft thick, of sand, silt, and clay, with locally notable organic content indicative of flood plain and shallow lacustrine settings; and (3) sandstone clast content that far exceeds the 17% observed in the Vashon-recessional ‘Brinnon’ delta perched above the mouth the Dosewallips River. We infer from the relative abundance of sandstone that Olympic drift in the map area is derived from alpine ice that mainly plucked sandstone bedrock from the headwaters of the Dosewallips basin while less effectively scouring the basalt-dominated bedrock lower in the basin. We infer from the lower sandstone content in the Vashon-recessional Brinnon delta that the Olympic core was probably not heavily glaciated during late Vashon time.

We interpret unit Qapo as the stratigraphic equivalent of the nonglacial unit Qc, which interfingers with unit Qapo near the eastern boundary of the Seabeck quadrangle and consists of lower-energy nonglacial deposits east of that. Normal paleomagnetic orientation of peaty mud interbeds at paleomagnetic sample sites N2 (sec. 27, T25N R1W) and N3 (sec.1, T25N R1W) suggests a post-Matuyama (Fig. 3) unit age above sea level. Analysis of pollen data from the same sites (Leopold, Univ. of Wash., written and oral commun., 2013) suggests a cool-temperate, nonglacial setting, with site N2 (based on sparse data) suggesting mixed conifer forest in which relative abundance of *Abies* (fir) hints at conditions cooler than today, and site N3 suggesting conifer forest much like that in the present Puget Lowland. We collected our pollen and paleomagnetic samples at both sites at or within a few feet of the base of the exposed section. In the Big Beef and Anderson Creek basins, unit Qapo is present both above and below multiple northern-sourced tills, and the upper exposures of unit Qapo are generally noticeably less weathered than its basal exposures. We are wary of correlating individual exposures of unit Qapo based on relative weathering, but have no doubt that the general downsection increase in weathering is broadly time-significant and consistent with the intervening record of multiple glaciations.

At date site GD5, sand (unit Qga$_p$) overlies a thin sheet of till (unit Qpt), which in turn overlies a thin seam of peat resting on sand of unknown thickness (unit Qapo)(composite columnar section on map). This suggests pre-Double Bluff age (older than MIS 6) for unit Qapo downsection of the till below GD5.

Upsection of date site GD5 in the same drainage, unit Qga_p is exposed below, and unit Qgt_p above, unit Qapo (columnar section). This implies interfingering with Possession advance outwash and deposition of unit Qapo during Possession ice advance and suggests an Olympic ice advance and sediment pulse ahead of a Cordilleran ice incursion. A >43,500 ^{14}C yr BP date from date site GD2 (sec. 13, T25N R1W; Table B1) in the same drainage is consistent with this age assignment. We attempted to use pollen analysis to confirm the paleoenvironmental association with a northern ice approach at date site GD2, but pollen results proved inconclusive (Leopold, written and oral communs., 2013). There is a map edge mismatch with the Wildcat Lake quadrangle (Tabor and others, 2011) west of Big Beef Creek (sec. 27, T25N R1W) where Tabor and others mapped Vashon advance deposits and we mapped unit Qapo.

Pre-Vashon Northern-Sourced Glacial Deposits

Qgt_p **Possession till**—Diamicton consisting of clay, silt, sand, pebbles, cobbles, and isolated boulders, typically supported by a hard, muddy, sandy matrix; brown to gray, ranging to tan; typically lightly weathered but includes unweathered exposures. Unit Qpt_p is compact, with well-developed facies resembling concrete. Clasts in unit $Qgt_p$are commonly striated and faceted, with subangular or rounded edges. The unit is unsorted and unstratified, but locally banded. The age of the unit is inferred to be 80 to 60 ka (MIS 4) based on the upsection presence of a single more recent (Vashon) drift (MIS 2) and downsection luminescence age control at date sites GD4 (sec. 30, T25N R1E), GD5 (sec. 13, T25N R1W), and GD6 (sec. 12, T25N R1W)(Tables B2 and B3).

Qga_p **Possession advance outwash**—Medium to fine grained sand, locally ranging to silt, with some exposures pebbly; most commonly light gray, with some exposures medium gray or light brown; compact. Most exposures are horizontally laminated or seemingly structureless, but some are gently crossbedded. Diverse plutonic and metamorphic pebble content, relatively thick, uniform and clean sand packages, and dominantly south- to east-directed paleocurrent indicators caused us to favor association with northern-sourced outwash (see also *Pleistocene Glacial and Nonglacial Deposits*, p. 14). Luminescence dates (Tables B2 and B3; Fig. D3) at date sites GD4 (sec. 30, T25N R1E) and GD5 (sec 13, T25N R1W) nominally indicate Whidbey interglaciation age (MIS 5), but even carefully selected Possession Drift samples can be affected by partial bleaching and then yield luminescence dates consistent with MIS 5, as was the case with our samples GD4 (and GD5, where quartz yielded no reportable OSL date), suggesting that the age statements for those analyses are excessive (Mahan, oral and written commun., 2013). We therefore favor a Possession age (MIS 4), with MIS 4 defined as ~80 to ~60 ka (Fig. 3). However, reinterpretation as Whidbey Formation (MIS 5) would be consistent with petrographic similarity to Cascade-sourced nonglacial alluvial sand of an ancestral Snohomish River, which was noted by Dragovich (oral commun., 2013). Upsection of date site GD5, unit Qapo separates unit Qga_p from overlying Possession till (unit Qpt_p)(composite columnar section on map). We interpret this stratigraphy as interfingering of distal Possession advance outwash sand with alpine outwash of unit Qapo, and sand facies within unit Qapo may include Qga_p in this area.

Qgd_p **Possession Drift, undivided**—Diamicton and sand to pebble gravel with minor silt; light brown to gray; coarsens upward from fine sand with dropstones and silt beds to pebble gravel and diamicton; dense to very dense and massive; clasts subrounded to rounded; moderately to well sorted and unsorted; moderately stratified and medium to thickly bedded. Deposits include metamorphic and granitic clasts with minor oxidation and weathering. The maximum inferred thickness of unit Qgd_p is about 100 ft on the Toandos Peninsula, where the unit is exposed along the bluffs of Hood Canal and Dabob Bay, stratigraphically above sediment inferred to be Whidbey Formation, unit Qc_w of Easterbrook and others (1967), and below deposits from the Olympia nonglacial interval (unit Qc_o; MIS 3). We inferred (sparse) exposures of slightly oxidized northern-sourced drift beneath unit Qc_o to be Possession Drift; however, they could be older. Possession Drift is thought to be 60 to 80 ka old, deposited during MIS 4 (Easterbrook and others, 1967).

Qpt **Pre-Vashon till**—Diamicton consisting of clay, silt, sand, pebbles, cobbles, and isolated boulders, typically supported by a hard, muddy, sandy matrix; brown to gray, ranging to tan; typically lightly

weathered but includes unweathered exposures and heavily weathered exposures. Two heavily weathered exposures are at significant site S4 (sec. 22, T25N R1W) at stream level and at paleomagnetic analysis site N1 (sec. 12, T25N R1W) just above the beach top, where till is exposed, but due to map scale and an apparent lateral facies change to glaciolacustrine or glaciomarine drift, is included in line unit Qpd. Unit Qpt is compact, with well-developed facies resembling concrete, although the exposures at sites S4 and N1 are weakened by weathering. Clasts in unit Qpt are commonly striated and faceted, with subangular or rounded edges. The unit is unsorted and unstratified, but locally banded. We tentatively associate the tills at sites S4 and N1 with northern-sourced ice advance(s) but acknowledge possible Olympic origin because, due to weathering and limited exposure, we were unable to extract enough identifiable clasts for confident assessment. (See unit Qpd, p. 21, for additional arguments for northern-sourced association at site N1.) The age of unit Qpt is unknown, and the unit includes deposits from multiple glaciations.

Qpog **Pre-Vashon outwash pebble gravel**—Pebble gravel and typically more than 5% silty to sandy or clayey matrix; locally includes beds or lenses of sand or mud; mostly weathered to reddish brown in exposed faces, but locally ranging to gray; clasts commonly weathered, but fresh clasts may be most numerous in some exposures; clasts typically well rounded and well sorted; compact. Bedding was poorly expressed in all observed exposures. Unit Qpog was identified as northern-sourced based on the presence of plutonic and metamorphic clasts—we estimated 19% diagnostically northern-sourced clasts at two sites with clast counts. The thickness of unit Qpog appears to be about 150 ft to the west of Big Beef Creek near the southern map boundary (NW¼SW¼ sec. 27, T25N R1W) and likely exceeds 50 ft east of date site GD3. Other exposures of the unit were included with units Qpd. Unit Qpog is stratigraphically constrained to pre-Vashon (but otherwise unknown) age by exposure below other pre-Vashon units, including pre-Vashon till (unit Qpt) west of Big Beef Creek. A radiocarbon-infinite date from delicate organic debris in silt, sand, and pebble gravel (unit Qpu) at radiocarbon date site GD3 (sec. 18, T25N R1E) requires a pre-Vashon age for the downsection exposures of unit Qpog. There is a map edge mismatch with the Wildcat Lake quadrangle (Tabor and others, 2011) east of Big Beef Creek (sec. 27, T25N R1W), where Tabor and others interpreted outwash as Vashon advance and we mapped it as pre-Vashon.

Qpos **Pre-Vashon outwash sand**—Sand, some exposures pebbly; medium to fine grained, locally ranging to silt; most commonly light gray, with some exposures medium gray or light brown; compact. Most exposures are horizontally laminated or seemingly structureless, but some are gently crossbedded. Sand mineralogy is generally quartzo-feldspathic, consistent with a northern source, but according to petrographic review by Dragovich (oral commun., 2013), in at least some instances, such as at date site GD6 (sec. 12, T25N R1W), it is similar to Snohomish River sand. Diverse plutonic and metamorphic pebble content, relatively thick, uniform, and clean sand packages, and mostly south- to east-directed paleocurrent indicators caused us to favor association with northern-sourced outwash (see also *Pleistocene Glacial and Nonglacial Deposits*, p. 14). Qpos unit thickness appears to exceed 150 ft in some areas (see cross section A–A′–A″), but the thickest mapped sections likely include outwash from more than one glaciation. Unit Qpos is widely mapped in the Poulsbo quadrangle and the Anderson Creek basin. Its absence farther west suggests that Olympic-sourced sediment, and perhaps the western limit of the Seattle basin, prevented deposition of the unit there.

We interpret unit Qpos as primarily distal lacustrine deposits and proglacial advance outwash associated with northern-sourced ice incursions, but the unit includes some flood-plain deposits, and some of the outwash is likely recessional. Association with multiple pre-Vashon tills was observed in some areas, such as the Anderson Creek basin (where some of the unit is mapped as subunit Qga_p, and the unit therefore spans multiple glaciations. It also includes deposits that previous mappers interpreted as Vashon advance outwash (see also *Pre-Vashon Sediment*, p. 4). We base our reassignment to pre-Vashon age on stratigraphic observations and, in some locations, new age control. For example, a luminescence age estimate at site GD6 (sec. 12, T25N R1W) constrains unit age at that site to Double Bluff age (MIS 6) or older, consistent with our stratigraphic interpretation that the deposit is overlain by at least four tills (composite columnar section on map), thus suggesting a Defiance glaciation (MIS 8) or older age. Elsewhere, the unit age is unconstrained (except where mapped as unit Qga_p but clearly includes multiple pre-Vashon glaciations. There are map edge mismatches with the Wildcat Lake quadrangle (Tabor and others, 2011) and the Suquamish quadrangle (Haugerud and Troost, 2011) west of Big Beef Creek

(sec. 27, T25N R1W) and northeast of Crouch Creek (secs. 1, 12, and 13, T25N R1E) where Tabor and others and Haugerud and Troost interpreted outwash as Vashon advance whereas we mapped it as pre-Vashon. Subdivided into:

Qpf **Pre-Vashon silt**—Silt, locally ranging to clay or sand, with rare dropstones; dark to pale gray, commonly bluish-gray, with some exposures ranging to brown; compact. Most exposures are horizontally laminated, but some appear structureless. Widespread recognition of unit Qpf in outcrops and well records at relatively consistent elevation across the Poulsbo quadrangle, most notably at about 200 ft (ranging from 150–250 ft) suggests laterally continuous stratigraphic breaks that partly motivated our reassignment of some deposits previously mapped as Vashon advance outwash to older units. Absence of recognition of units Qpof and Qpos in most of the Seabeck quadrangle suggests that Olympic-sourced sediment, and perhaps the western limit of the Seattle basin, prevented deposition of the units there. Unit Qpf is undated and appears to include deposits from multiple glaciations. There is a map edge mismatch with the Suquamish quadrangle (Haugerud and Troost, 2011) at the northeast map corner (sec. 13, T26N R1E) where Haugerud and Troost interpreted the outwash as Vashon-age sand.

Qpd **pre-Vashon drift**—Till and outwash consisting of cobble to pebble gravel with occasional boulders and a sandy to clayey matrix; combines units Qpt, Qpog, Qpos, and Qpf and is shown where map scale or limited exposures prevented separate mapping of the component units. We favor northern origin for unit Qpd at paleomagnetic sample site N1 (sec. 12, T25N R1W), partly because it includes basal outwash pebble gravel with granitic clasts. We were unable to extract enough identifiable clasts to permit confident source determination from overlying till at the site, but the till appears to laterally grade to—but may instead be overlain by—glaciomarine or glaciolacustrine drift, and we think that in this location a northern ice advance would be more likely than an Olympic ice advance to result in a floating ice margin. Unit Qpd at site N1 is stratigraphically below date site GD6 (composite columnar section on map; Tables B2 and B3) and therefore is of Defiance glaciation (MIS 8) or older age at this site. Our stratigraphic interpretation of the overlying section (columnar section) suggests that it pre-dates MIS 8. Elsewhere the unit age is indeterminate but pre-Vashon. Glaciomarine or glaciolacustrine mud associated with the till at site N1 revealed paleomagnetically normal orientation, suggesting a post-Matuyama (or pre-Matuyama magnetically normal) age. Since the tills associated with site N1and significant site S4 are the stratigraphically lowest, and by far the most weathered we observed in the map area, we suspect that all sediment above sea level in the map area post-dates the Matuyama reversed chron (Fig. 3).

Pre-Vashon Nonglacial Deposits

Qc_o **Pre-Vashon alluvium of the Olympia nonglacial interval**—Sand, silt, pebble gravel, clay, peat, and organic debris; mostly gray to tan, locally brown, with silt and clay facies ranging to bluish-gray; compact. Unit Qc_o is mapped as an Olympia-age member of unit Qc where age control supports Olympia nonglacial age (MIS 3). A late Olympia age for the unit is supported by a 16,510 ±320 ^{14}C yr BP date on wood from date site GD7 east of Dyes Inlet (sec. 21, T25N R1E; Table B1; Deeter, 1979; OxCal 2σ age 20.360–18.922 ka) and a 35,210 ±320 ^{14}C yr BP date on unidentified organics from a paleosol at date site GD14 on the Toandos Peninsula (sec. 4, T25N R1W; Table B1). A >45,000 ^{14}C yr BP date on gyttja is consistent with MIS 3 age at date site GD13, also on the Toandos Peninsula, where MIS 3 age is also supported by correlation to a 47 ka luminescence date 4 mi north of the map area (Contreras and others, 2013). Correlation to strata with a 73 ka luminescence date (IRSL) and radiocarbon finite dates in the adjacent Lofall quadrangle (Contreras and others, 2013) support MIS 3 age for deposits exposed in drainages west of site HVSR 11 (sec. 16, T26N R1E) on the Kitsap Peninsula. Pollen analysis of organic-rich mud from date site GD7 suggests a paleoclimate cooler than the modern setting (Leopold, written and oral commun., 2013). Possible faulting at GD7 is discussed above (see *Other Observations with Potential Structural Significance*, p. 11).

Qcw **Whidbey Formation**—Silt, clay, and sand; light-gray to light-brown; dense and stiff; clasts typically subangular to subrounded; well stratified and well sorted; thinly laminated to very thickly bedded. Organic material within the unit is locally noted in well reports. Unit Qcw appears to have a maximum thickness of about 200 ft on the Toandos Peninsula, where we infer tectonic uplift along portions of the DBFZ. It appears to represent nonglacial prodelta deposits that received sand, silt, and clay from the north and east. Contact relations are unclear, but well reports and rare exposures suggest thin, discontinuous, oxidized northern-sourced glacial drift, which we infer to be Possession Drift (MIS 4), above unit Qcw. The deposits within unit Qcw suggest a low-energy depositional setting, graded to base level. The exposure elevations up to 200 ft above modern sea level suggest a significantly more distant shore than that present in the modern environment. A hypothetical channel slope of 0.001 (probably excessively steep) along a 30-mi-long, straight line northwest from the central Toandos Peninsula to the mouth of the Dungeness River (probably too short a distance to reach that location) would yield a 160 ft elevation drop; a 100-mi river length at the same slope would yield a 528 ft elevation drop. One possible—but probably unnecessary—scenario is tectonic uplift in addition to aggradation. We lack direct age control for this unit within the map area and therefore rely on sparse age data from upsection unit Qco (this study) and stratigraphic layering to assign the deposits in this unit to the Whidbey interglaciation (MIS 5). We further note similarity in character and exposure elevation to deposits mapped as Whidbey Formation south of the map area, where two samples yielded three luminescence age estimates between 82.5 ±3.89 ka and 133 ±9.74 ka (Contreras and others, 2012a,b). These dates correspond to dates provided by Easterbrook (1994) for the Whidbey Formation.

Qc **Pre-Vashon alluvium**—Sand, silt, pebble gravel, clay, peat, and organic sediment; mostly gray to tan, locally brown, with silt and clay facies ranging to bluish-gray; compact; moderately sorted; bedded. Unit Qc is the lateral facies change from unit Qapo in the southwest of the map area to finer-grained, more distinctly nonglacial, lower-energy flood plain deposits that dominate nonglacial deposits farther north and in the center of the Puget Lowland. Bedding in unit Qc is mostly horizontal and planar or low-angle crossbedded. We saw few exposures of pre-Vashon peat or woody debris in the map area and included most in unit Qc. Well and boring logs more commonly noted them and contributed to our interpretation of unit Qc as nonglacial. Where organic matter was not noted, we typically had little basis for distinction among the sand, silt, and clay facies of units Qc, Qpos, and Qpf, and we suspect that some of each may be misidentified. At paleomagnetic sample site N4 (sec. 20, T25N R1E) undated but paleomagnetically normal sand, mud, peat, and pebble gravel of unit Qc are folded, broken, offset, and penetrated by injection features, contributing to our mapping of DBFZ fault 2 there (see also *Quaternary Structure and Neotectonics*, p. 7). Analysis of a pollen sample from these deposits proved paleo-environmentally inconclusive (Leopold, written and oral communs., 2013). Similar deposits east of Dyes Inlet at date site GD7 and paleomagnetic sample site N5 (secs. 20 and 27, T25N R1E) were mapped as subunit Qco, based on a radiocarbon date there (Deeter, 1979).

Glacial and Nonglacial Deposits, Undivided

Qpu **Undivided Quaternary sediment older than Vashon till**—Sand, pebble gravel, silt, clay, diamicton, organic sediment, and boulders; color and weathering variable; compact; varied grain size, rounding, sorting, and bedding. Shown where sediment age, paleoenvironmental association, and sources were unconstrained or enigmatic, as at date site GD3 (sec. 18, T25N R1E), where an upward-coarsening section, bluish-gray color, and a near-absence of pollen (Leopold, written and oral commun., 2013) favored glacial association, but the presence of a thin sheet of detrital organic debris favored a nonglacial setting. The radiocarbon date (>43,500 yr BP, Table B1), sampled only a few feet downsection from surficial diamicton (mapped as unit Qgic), contributed to our inference that in this map area most subsurface deposits, even shallow ones, are of pre-Vashon age. Pollen analysis from the peaty top of unit Qpu at the site proved paleo-environmentally inconclusive. There is a map edge mismatch with the Wildcat Lake quadrangle (Tabor and others, 2011) at the southwestern map corner where Tabor and others included older sediment exposed in the valley wall southwest of Stavis Bay with valley floor alluvium (unit Qal), but we identified older units upslope.

Tertiary Sedimentary and Volcanic Bedrock

Em **Marine sedimentary rocks (middle Eocene)**—Marine silty sandstone, siltstone, and boulder conglomerate; green-gray to light brown; fine to coarse grained; grains and clasts dominantly basaltic; moderately well rounded; moderately well sorted and well bedded; thinly bedded to massive. The unit is 236 ft thick at Pulali Point as measured by Squires and others (1992) and appears to overlie Crescent Formation (unit Evc) along an angular unconformity or fault. We suggest the possibility of the contact being a fault because it is slickensided. Unit Em at Pulali Point is fossiliferous and includes benthic foraminifers of Narizian stage (Squires and others, 1992). The unit is Eocene in age according to Squires and others, who, based on proximity, suggested possible correlation of the Pulali Point section to known exposures of Aldwell Formation on the west shore of Quilcene Bay, or to Humptulips Formation. Narizian Stage (to reworked? Ulatisian Stage) microfossils and macrofossils suggest a middle Eocene unit age at date site GD10 (Pulali Point, sec. 18, T26N R1W) (Squires and others, 1992). Squires and others estimated that age at 52 Ma, but Armentrout and others (1983) and Elizabeth Nesbitt (Univ. of Wash., written commun., 2013) suggested that the Narizian Stage is younger, with Nesbitt indicating "~ 48 to 38 Ma" for the Pulali Point exposure. McDougall (2008) estimated a middle to late Eocene, 35 to 42.6 Ma age for the Narizian Stage type section in California, although Nesbitt cautioned (written commun., 2013) that correlation of the Pacific Northwest Stages with those defined in California are problematic.

Evc **Crescent Formation (early to middle Eocene)**—Basalt; black to greenish black where fresh, weathers gray and medium yellow-brown; commonly occurs as fine-grained sills and flows; commonly includes amygdules of zeolite and chlorite-group minerals. Flows include rare columns, vesicles, and scoria. This unit typically includes plagioclase with intergrowths of pyroxenes and disseminated opaque minerals. Replacement of interstitial glass by chlorite and oxidation products is also common. Unit Evc, as mapped by Tabor and Cady (1978), is exposed in the northwest corner of the map area at Pulali and Wawa Points, where it is covered with glacial deposits except along the shore and is in unconformable contact with upsection sedimentary rocks (unit Em). Babcock obtained a $^{40}Ar/^{39}Ar$ date of 50.5 ±1.6 Ma on a basalt flow from about 620 ft below the top of the Crescent Formation exposure at Pulali Point (date site GD11; sec. 18, T26N R1W)(Squires and others, 1992; Hirsch and Babcock, 2009; additional details provided by Polenz and others, 2012c). Squires and others (1992) suggested that the date may represent intrusion of a sill because they thought that upsection biostratigraphic control suggests a greater (than 50.5 Ma) age for upsection sedimentary rocks, but their biostratigraphic age estimate differs from that of Armentrout and others (1983) or more recent evaluation by Nesbitt (written commun., 2013) and may also conflict with age control for the Narizian type section in California (see also unit Em).

ACKNOWLEDGMENTS

This geologic map was funded in part by the USGS National Cooperative Geologic Mapping Program under award no. G12AC20234. We thank Randall Conger-Best for assistance with thin section petrographic sample analysis, subsurface data compilation, preparation, and interpretation, assistance with write-up, and other tasks; Shannon Mahan and Harrison Gray (U.S. Geological Survey) for analysis of luminescence samples; Estella Leopold (Univ. of Wash.) for pollen sample review and interpretation; Linda Dancey and James White (Natural Resources Canada) for pollen sample preparation; Elizabeth Nesbitt (Univ. of Wash.) for assistance with bedrock fossil content and ages; Beth Novak and Bernard Housen (Western Wash. Univ.) for paleomagnetic sample analysis; Beta Analytic and Direct AMS for radiocarbon analytical services; Kitsap County and the Jefferson County Assessor's Office for GIS data; Joe Becker, Michael Krautkramer, and Aaron Young (Robinson Noble, Inc.), for assistance with reports and well records; the Wash. State Dept. of Transportation for access to and Eric Dingeldein for assistance with WSDOT geotechnical records; Rex Crawford and Joe Rocchio (Wash. State Dept. of Natural Resources) for assistance with wood sample species identification; Brian Sherrod (U.S. Geological Survey) for collaborative interpretation of data and samples from a relict peat deposit at Dyes Inlet; Richard Blakely (U.S. Geological Survey) for aeromagnetic field strength maps; Andy Lamb (Boise State Univ.) for magnetic, gravity, seismic line, and other data; Thomas Pratt (USGS) and Bill Lingley (Leslie Geological Services) for assistance with interpretation of seismic survey data; Bob Carson (Whitman College) for sharing his field notes and knowledge of the area; Glenn Thackray (Idaho State

Univ.) and Wendy Gerstel (Qwg Applied Geology) for insights into glaciations of the Olympic Mountains; Ana Shafer (Wash. Dept. of Natural Resources) for landslide data; Wash. Div. of Geology and Earth Resources staff Bryan Garcia, Rian Skov, Coire McCabe, Nick Hehemann; Eli Newby, and Carrie Gillum for field and boat help. We thank countless landowners for sharing local knowledge and permitting us to map on their land.

REFERENCES CITED

Anundsen, Karl; Abella, S. E. B.; Leopold, E. B.; Stuiver, M.; Turner, S., 1994, Late-glacial and early Holocene sea-level fluctuations in the central Puget Lowland, Washington, inferred from lake sediments: Quaternary Research, v. 42, no. 2, p. 149-161.

Armentrout, J. M.; Hull, D. A.; Beaulieu, J. D.; Rau, W. W., 1983, Correlation of Cenozoic stratigraphic units of western Oregon and Washington: Oregon Department of Geology and Mineral Industries Oil and Gas Investigation 7, 90 p., 1 plate.

Atwater, B. F., 1999, Radiocarbon dating of a Seattle earthquake to A.D. 900-930 [abstract]: Seismological Research Letters, v. 70, no. 2, p. 232.

Birdseye, R. U., 1976, Geologic map of east-central Jefferson County, Washington: Washington Division of Geology and Earth Resources Open File Report 76-26, 1 sheet, scale 1:24,000. [http://www.dnr.wa.gov/publications/ger_ofr76-26_geologic_map_jefferson_co_24k.pdf]

Blakely, R. J.; Sherrod, B. L.; Hughes, J. F.; Anderson, M. L.; Wells, R. E.; Weaver, C. S., 2009, Saddle Mountain fault deformation zone, Olympic Peninsula, Washington—Western boundary of the Seattle uplift: Geosphere, v. 5, no. 2, p. 105-125.

Blakely, R. J.; Sherrod, B. L.; Weaver, C. S.; Wells, R. E.; Rohay, A. C.; Barnett, E. A.; Knepprath, N. E., 2011, Connecting the Yakima fold and thrust belt to active faults in the Puget Lowland, Washington: Journal of Geophysical Research, v. 116, B07105, 33 p.

Blakely, R. J.; Wells, R. E.; Weaver, C. S.; Johnson, S. Y., 2002, Location, structure, and seismicity of the Seattle fault zone, Washington—Evidence from aeromagnetic anomalies, geologic mapping, and seismic-reflection data: Geological Society of America Bulletin, v. 114, no. 2, p. 169-177.

Booth, D. B., 1994, Glaciofluvial infilling and scour of the Puget Lowland, Washington, during ice-sheet glaciation: Geology, v. 22, no. 8, p. 695-698.

Booth, D. B.; Troost, K. G.; Clague, J. J.; Waitt, R. B., 2004, The Cordilleran ice sheet. *In* Gillespie, A. R.; Porter, S. C.; Atwater, B. F., editors, The Quaternary period in the United States: Elsevier, p. 17-43.

Borchardt, G. A.; Aruscavage, P. J.; Millard, H. T., Jr., 1972, Correlation of the Bishop ash, a Pleistocene marker bed, using instrumental neutron activation analysis: Journal of Sedimentary Petrology, v. 42, no. 2, p. 301-306.

Bretz, J H., 1910, Glacial lakes of Puget Sound—Preliminary paper: Journal of Geology, v. 18, no. 5, p. 448-458.

Bretz, J H., 1913, Glaciation of the Puget Sound region: Washington Geological Survey Bulletin 8, 244 p., 3 plates. [http://www.dnr.wa.gov/publications/ger_b8_glaciation_pugetsound.pdf]

Brocher, T. M.; Blakely, R. J.; Wells, R. E., 2004, Interpretation of the Seattle uplift, Washington, as a passive-roof duplex: Seismological Society of America Bulletin, v. 94, no. 4, p. 1379-1401.

Brocher, T. M.; Parsons, T. E.; Blakely, R. J.; Christensen, N. I.; Fisher, M. A.; Wells, R. E.; SHIPS Working Group, 2001, Upper crustal structure in Puget Lowland, Washington—Results from the 1998 seismic hazards investigations in Puget Sound: Journal of Geophysical Research, v. 106, no. B7, p. 13,541-13,564.

Bronk Ramsey, Christopher, 2009, Bayesian analysis of radiocarbon dates: Radiocarbon, v. 51, no. 1, p. 337-360.

Bucknam, R. C.; Hemphill-Haley, Eileen; Leopold, E. B., 1992, Abrupt uplift within the past 1700 years at southern Puget Sound, Washington: Science, v. 258, no. 5088, p. 1611-1614.

Carson, R. J., 1975, Late Quaternary deformation on the southern Toandos Peninsula, Jefferson County, Wash. [abstract]: Northwest Scientific Association, 48th Annual Meeting, Program and Abstracts, abstract no. 69.

Contreras, T. A.; Spangler, Eleanor; Fusso, L. A.; Reioux, D. A.; Paulin, Gabriel Legorreta; Pringle, P. T.; Carson, R. J.; Lindstrum, E. F.; Clark, K. P.; Tepper, J. H.; Pileggi, Domenico; Mahan, S. A., 2012a, Geologic map of the Eldon 7.5-minute quadrangle, Jefferson, Kitsap, and Mason Counties, Washington: Washington Division of Geology and Earth Resources Map Series 2012-03, 1 sheet, scale 1:24,000, with 60 p. text. [http://www.dnr.wa.gov/publications/ger_ms2012-03_geol_map_eldon_24k.zip]

Contreras, T. A.; Stone, K. A; Legorreta Paulin, Gabriel, 2013, Geologic map of the Lofall 7.5-minute quadrangle, Jefferson and Kitsap Counties, Washington: Washington Division of Geology and Earth Resources Map Series 2013-03, 1 sheet, scale 1:24,000, with 19 p. text. [http://www.dnr.wa.gov/publications/ger_ms2013-03_geol_map_lofall_24k.zip]

Contreras, T. A.; Weeks, S. A.; Stanton, K. M. D.; Stanton, B. W.; Perry, B. B.; Walsh, T. J.; Carson, R. J.; Clark, K. P.; Mahan, S. A., 2012b, Geologic map of the Holly 7.5-minute quadrangle, Jefferson, Kitsap, and Mason Counties, Washington: Washington Division of Geology and Earth Resources Open File Report 2011-5, 1 sheet, scale 1:24,000, with 13 p. text. [http://www.dnr.wa.gov/publications/ger_ofr2011-5_geol_map_holly_24k.zip]

Dadisman, S. V.; Johnson, S. Y.; Childs, J. R., 1997, Marine, high-resolution, multichannel, seismic-reflection data collected during Cruise G3-95-PS, northwestern Washington: U.S. Geological Survey Open-File Report 97-735, 3 CD-ROM disks.

Daneš, Z. F.; Bonno, M.; Brau, J. E.; Gilham, W. D.; Hoffman, T. F.; Johansen, D.; Jones, M. H.; Malfait, Bruce; Masten, J.; Teague, G. O., 1965, Geophysical investigation of the southern Puget Sound area, Washington: Journal of Geophysical Research, v. 70, no. 22, p. 5573-5580.

Deeter, J. D., 1979, Quaternary geology and stratigraphy of Kitsap County, Washington: Western Washington University Master of Science thesis, 175 p., 1 plate, scale 1:42,000.

Dethier, D. P.; Pessl, Fred, Jr.; Keuler, R. F.; Balzarini, M. A.; Pevear, D. R., 1995, Late Wisconsinan glaciomarine deposition and isostatic rebound, northern Puget Lowland, Washington: Geological Society of America Bulletin, v. 107, no. 11, p. 1288-1303.

Domack, E. W., 1983, Facies of late Pleistocene glacial-marine sediments on Whidbey Island, Washington—An isostatic glacial-marine sequence. *In* Molnia, B. F., editor, Glacial-marine sedimentation: Plenum Press, p. 535-570.

Dragovich, J. D., 2007, Sand point count and geochemical data in the Fall City and Carnation 7.5-minute quadrangles, King County, Washington: Washington Division of Geology and Earth Resources Open File Report 2007-3, zip archive containing 4 files: Microsoft Word, Microsoft Excel, and Adobe PDF formats, 386 kb. [http://www.dnr.wa.gov/Publications/ger_ofr2007-3_fallcity_supplement.zip]

Dragovich, J. D.; Anderson, M. L.; MacDonald, J. H., Jr.; Mahan, S. A.; DuFrane, S. A.; Littke, H. A.; Wessel, G. R.; Saltonstall, J. H.; Koger, C. J.; Cakir, Recep, 2010a, Supplement to the geologic map of the Carnation 7.5-minute quadrangle, King County, Washington—Geochronologic, geochemical, point count, geophysical, earthquake, fault, and neotectonic data: Washington Division of Geology and Earth Resources Open File Report 2010-2, zip archive containing 9 files: Microsoft Word, Microsoft Excel, and Adobe PDF formats, 24.7 MB. [http://www.dnr.wa.gov/publications/ger_ofr2010-2_carnation_supplement.zip]

Dragovich, J. D.; Anderson, M. L.; Mahan, S. A.; MacDonald, J. H., Jr.; McCabe, C. P.; Cakir, Recep; Stoker, B. A.; Villeneuve, N. M.; Smith, D. T.; Bethel, J. P., 2012, Geologic map of the Lake Joy 7.5-minute quadrangle, King County, Washington: Washington Division of Geology and Earth Resources Map Series 2012-01, 2 sheets, scale 1:24,000, 79 p. text. [http://www.dnr. wa.gov/publications/ger_ms2012-01_geol_map_lake_joy_24k.zip]

Dragovich, J. D.; Anderson, M. L.; Walsh, T. J.; Johnson, B. L.; Adams, T. L., 2007, Geologic map of the Fall City 7.5-minute quadrangle, King County, Washington: Washington Division of Geology and Earth Resources Geologic Map GM-67, 1 sheet, scale 1:24,000. [http://www.dnr.wa.gov/publications/ger_gm67_geol_map_fallcity_24k.zip]

Dragovich, J. D.; Littke, H. A.; Anderson, M. L.; Wessel, G. R.; Koger, C. J.; Saltonstall, J. H.; MacDonald, J. H., Jr.; Mahan, S. A.; DuFrane, S. A., 2010b, Geologic map of the Carnation 7.5-minute quadrangle, King County, Washington: Washington Division of Geology and Earth Resources Open File Report 2010-1, 1 sheet, scale 1:24,000, 21 p. text. [http://www.dnr.wa.gov/publications/ger_ofr2010-1_geol_map_carnation_24k.zip]

Dragovich, J. D.; Pringle, P. T.; Walsh, T. J., 1994, Extent and geometry of the mid-Holocene Osceola mudflow in the Puget Lowland—Implications for Holocene sedimentation and paleogeography: Washington Geology, v. 22, no. 3, p. 3-26. [http://www.dnr.wa.gov/publications/ger_washington_geology_1994_v22_no3.pdf]

Easterbrook, D. J., 1994, Chronology of pre-late Wisconsin Pleistocene sediments in the Puget Lowland, Washington. *In* Lasmanis, Raymond; Cheney, E. S., convenors, Regional geology of Washington State: Washington Division of Geology and Earth Resources Bulletin 80, p. 191-206.

Easterbrook, D. J.; Crandell, D. R.; Leopold, E. B., 1967, Pre-Olympia Pleistocene stratigraphy and chronology in the central Puget Lowland, Washington: Geological Society of America Bulletin, v. 78, no. 1, p. 13-20.

Eronen, Matti; Kankainen, Tuovi; Tsukada, Matsuo, 1987, Late Holocene sea-level record in a core from the Puget Lowland, Washington: Quaternary Research, v. 27, no. 2, p. 147-159.

Gower, H. D.; Yount, J. C.; Crosson, R. S., 1985, Seismotectonic map of the Puget Sound region, Washington: U.S. Geological Survey Miscellaneous Investigations Series Map I-1613, 1 sheet, scale 1:250,000, with 15 p. text.

Grimstad, Peder; Carson, R. J., 1981, Geology and ground-water resources of eastern Jefferson County, Washington: Washington Department of Ecology Water-Supply Bulletin 54, 125 p., 3 plates. [http://www.ecy.wa.gov/programs/eap/wsb/wsb_All.html]

Hallet, D. J.; Hills, L. V.; Clague, J. J., 1997, New accelerator mass spectrometry radiocarbon ages for the Mazama tephra layer from Kootenay National Park, British Columbia, Canada: Canadian Journal of Earth Sciences, v. 34, p. 1202-1209.

Harding, T. P., 1974, Petroleum traps associated with wrench faults: American Association of Petroleum Geologists Bulletin, v. 58, no. 7, p. 1290-1304.

Haug, B. J., 1998, High resolution seismic reflection interpretations of the Hood Canal–Discovery Bay fault zone, Puget Sound, Washington: Portland State University Master of Science thesis, 1 v.

Haugerud, R. A., 2009, Preliminary geomorphic map of the Kitsap Peninsula, Washington: U.S. Geological Survey, Open-File Report 2009-1033, 2 sheets, scale 1:36,000. [http://pubs.usgs.gov/of/2009/1033/]

Haugerud, R. A.; Troost, K. G., 2011, Geologic map of the Suquamish 7.5′ quadrangle and part of the Seattle North 7.5′ x 15′ quadrangle, Kitsap County, Washington: U.S. Geological Survey Scientific Investigations Map 3181, 1 plate, scale 1:24,000, with 9 p. text. [http://pubs.usgs.gov/sim/3181/]

Hirsch, D. M.; Babcock, R. S., 2009, Spatially heterogeneous burial and high-P/T metamorphism in the Crescent Formation, Olympic Peninsula, Washington: American Mineralogist, v. 94, no. 8-9, p. 1103-1110.

Johnson, S. Y.; Blakely, R. J.; Stephenson, W. J.; Dadisman, S. V.; Fisher, M. A., 2004, Active shortening of the Cascadia forearc and implications for seismic hazards of the Puget Lowland: Tectonics, v. 23, TC1011, doi:10.1029/2003TC001507, 2004, 27 p.

Johnson, S. Y.; Potter, C. J.; Armentrout, J. M.; Miller, J. J.; Finn, C. A.; Weaver, C. S., 1996, The southern Whidbey Island fault—An active structure in the Puget Lowland, Washington: Geological Society of America Bulletin, v. 108, no. 3, p. 334-354, 1 plate.

Kahle, S. C., 1998, Hydrogeology of Naval Submarine Base Bangor and vicinity, Kitsap County, Washington: U.S. Geological Survey Water-Resources Investigations Report 97-4060, 107 p., 7 plates. [http://pubs.er.usgs.gov/usgspubs/wri/wri974060]

Kelsey, H. M.; Sherrod, B. L.; Nelson, A. R.; Brocher, T. M., 2008, Earthquakes generated from bedding plane-parallel reverse faults above an active wedge thrust, Seattle fault zone: Geological Society of America Bulletin, v. 120, no. 11-12, p. 1581-1597.

Kimball, J. P., 1897, Physiographic geology of the Puget Sound basin [in 2 parts]: American Geologist, v. 19, no. 4, p. 225-237 [part 1]; v. 19, no. 5, p. 304-322 [part 2].

Kramer, S. L., 1996, Geotechnical earthquake engineering: Prentice Hall, 653 p.

Lamb, A. P.; Liberty, L. M.; Blakely, R. J.; Pratt, T. L.; Sherrod, B. L.; van Wijk, K., 2012, Western limits of the Seattle fault zone and its interaction with the Olympic Peninsula, Washington: Geosphere, v. 8, no. 3, doi: 10.1130/GESoo780.1.

Lane, J. W., Jr.; White, E. A.; Steele, G. V.; Cannia, J. C., 2008, Estimation of bedrock depth using the horizontal-to-vertical (H/V) ambient-noise seismic method. *In* Symposium on the Application of Geophysics to Engineering and Environmental Problems, April 6-10, 2008, Philadelphia, Pennsylvania, Proceedings: Denver, Colorado, Environmental and Engineering Geophysical Society, 13 p. [http://water.usgs.gov/ogw/bgas/publications/SAGEEP2008-Lane_HV/SAGEEP2008-Lane_HV.pdf]

Laprade, W. T., 2003, Subglacially reworked till in the Puget Lowland [abstract]: Geological Society of America Abstracts with Programs, v. 35, no. 6, p. 216.

Logan, R. L.; Walsh, T. J., 2009, Mima Mounds formation and their implications for climate change [abstract]. *In* Northwest Scientific Association, The Pacific Northwest in a changing environment—Northwest Scientific Association 81st annual meeting; Program with abstracts: Northwest Scientific Association, p. 38-39.

Mace, C. G.; Keranen, K. M., 2012, Oblique fault systems crossing the Seattle basin—Geophysical evidence for additional shallow fault systems in the central Puget Lowland: Journal of Geophysical Research, v. 117, B03105, 19 p.

McDougall, Kristin, 2007, California Cenozoic biostratigraphy—Paleogene. *In* Hosford Scheirer, Allegra, editor, 2007, Petroleum Systems and geologic assessment of oil and gas in the San Joaquin Basin Province, California: U.S. Geological Survey Professional Paper 1713. [http://pubs.usgs.gov/pp/pp1713/]

McKenna, J. P.; Lidke, D. J.; Coe, J. A., 2008, Landslides Mapped from LIDAR Imagery, Kitsap County, Washington: U.S. Geological Survey Open-File Report 2008-1292, 1 sheet, scale 1:50,000, 81 p. text. [http://pubs.usgs.gov/of/2008/1292/]

Micromed s.p.a., 2012, Introduction to the H/V modeling routine for stratigraphic purposes in *Grilla*, v. 3.0: Micromed s.p.a., 21 p. [http://tromino.eu/]

Mosher, D. C.; Hewitt, A. T., 2004, Late Quaternary deglaciation and sea-level history of eastern Juan de Fuca Strait, Cascadia: Quaternary International, v. 121, no. 1, p. 23-39.

Myers, J. N., 2011, NW Stavis Bay Road bridge replacement, mile post 2.00 to 2.13, contract provisions, Kitsap County Department of Public Works County Road Project No. 3640: Myers Biodynamics, Inc., Project No. 091430-5 [prepared for Kitsap County Department of Public Works], 17 p.

Paterson, W. D., 1981, Ground water hydrology at the Naval Submarine Base Bangor, Washington: Robinson, Noble & Carr, Inc., 2 v., 123 p., 3 plates.

Pettijohn, F. J., 1957, Sedimentary rocks: Harper and Brothers, 718 p.

Polenz, Michael; Alldritt, Katelin; Heheman, N. J.; Logan, R. L., 2009a, Geologic map of the Burley 7.5-minute quadrangle, Kitsap and Pierce Counties, Washington: Washington Division of Geology and Earth Resources Open File Report 2009-8, 1 sheet, scale 1:24,000. [http://www.dnr.wa.gov/publications/ger_ofr2009-8_geol_map_burley_24k.pdf]

Polenz, Michael; Alldritt, Katelin; Heheman, N. J.; Sarikhan, I. Y.; Logan, R. L., 2009b, Geologic map of the Belfair 7.5-minute quadrangle, Mason, Kitsap, and Pierce Counties, Washington: Washington Division of Geology and Earth Resources Open File Report 2009-7, 1 sheet, scale 1:24,000. [http://www.dnr.wa.gov/publications/ger_ofr2009-7_geol_map_belfair_24k.pdf]

Polenz, Michael; Contreras, T. A.; Czajkowski, J. L.; Legorreta Paulin, Gabriel; Miller, B. A.; Martin, M. E.; Walsh, T. J.; Logan, R. L.; Carson, R. J.; Johnson, C. N.; Skov, R. H.; Mahan, S. A.; Cohan, C. R., 2010a, Supplement to geologic maps of the Lilliwaup, Skokomish Valley, and Union 7.5-minute quadrangles, Mason County, Washington—Geologic setting and development around the Great Bend of Hood Canal: Washington Division of Geology and Earth Resources Open File Report 2010-5, 27 p. [http://www.dnr.wa.gov/publications/ger_ofr2010-5_lilliwaup_skokomish_valley_union_suppl_24k.pdf]

Polenz, Michael; Czajkowski, J. L.; Legorreta Paulin, Gabriel; Contreras, T. A.; Miller, B. A.; Martin, M. E.; Walsh, T. J.; Logan, R. L.; Carson, R. J.; Johnson, C. N.; Skov, R. H.; Mahan, S. A.; Cohan, C. R., 2011, Geologic map of the Skokomish Valley and Union 7.5-minute quadrangles, Mason County, Washington: Washington Division of Geology and Earth Resources Open File Report 2010-3 revised, 21 p., 1 plate, scale 1:24,000. [http://www.dnr.wa.gov/publications/ger_ofr2010-3_geol_map_skokomish_valley_union_24k.zip]

Polenz, Michael; Miller, B. A.; Davies, Nigel; Perry, B. B.; Clark, K. P.; Walsh, T. J.; Carson, R. J.; Hughes, J. F., 2012a, Geologic map of the Hoodsport 7.5-minute quadrangle, Mason County, Washington: Washington Division of Geology and Earth Resources Open File Report 2011-3, 1 sheet, scale 1:24,000, with 16 p. text. [http://www.dnr.wa.gov/Publications/ger_ofr2011-3_geol_map_hoodsport_24k.zip]

Polenz, Michael; Miller, B. A.; Davies, Nigel; Perry, B. B.; Hughes, J. F.; Clark, K. P.; Walsh, T. J.; Tepper, J. H.; Carson, R. J., 2012b, Analytical data from the Hoodsport 7.5-minute quadrangle, Mason County, Washington—Supplement to Open File Report 2011-3: Washington Division of Geology and Earth Resources Open File Report 2011-4, 42 p. [http://www.dnr.wa.gov/Publications/ger_ofr2011-4_hoodsport_supplement.pdf]

Polenz, Michael; Spangler, Eleanor; Fusso, L. A.; Reioux, D. A.; Cole, R. A.; Walsh, T. J.; Cakir, Recep; Clark, K. P.; Tepper, J. H.; Carson, R. J.; Pileggi, Domenico; Mahan, S. A., 2012c, Geologic map of the Brinnon 7.5-minute quadrangle, Jefferson and Kitsap Counties, Washington: Washington Division of Geology and Earth Resources Map Series 2012-02, 1 sheet, scale 1:24,000, with 47 p. text. [http://www.dnr.wa.gov/publications/ger_ms2012-02_geol_map_brinnon_24k.zip]

Porter, S. C.; Carson, R. J., 1971, Problems of interpreting radiocarbon dates from dead-ice terrain, with an example from the Puget Lowland of Washington: Quaternary Research, v. 1, no. 3, p. 410-414.

Porter, S. C.; Swanson, T. W., 1998, Radiocarbon age constraints on rates of advance and retreat of the Puget lobe of the Cordilleran ice sheet during the last glaciation: Quaternary Research, v. 50, no. 3, p. 205-213.

Prescott, J. R.; Hutton, J. T., 1994, Cosmic ray contribution to dose rates for luminescence and ESR dating—Large depths and long-term time variations: Radiation Measurements, v. 23, no. 2-3, p. 497-500.

Raisz, E. J., 1945, The Olympic–Wallowa lineament: American Journal of Science, v. 243A [Daly volume], p. 479-485. [http://earth.geology.yale.edu/~ajs/1945A/479.pdf]

Sanderson, D. J.; Marchini, W. R. D., 1984, Transpression: Journal of Structural Geology, v. 6, no. 5, p. 449-458.

Sarikhan, I. Y.; Stanton, K. D.; Contreras, T. A.; Polenz, Michael; Powell, Jack; Walsh, T. J.; Logan, R. L., 2008, Landslide reconnaissance following the storm event of December 1–3, 2007, in western Washington: Washington Division of Geology and Earth Resources Open File Report 2008-5, 16 p. [http://www.dnr.wa.gov/publications/ger_ofr2008-5_dec2007_landslides.pdf]

Sherrod, B. L.; Blakely, R. J.; Weaver, C. S.; Kelsey, H. M.; Barnett, Elizabeth; Liberty, Lee; Meagher, K. L.; Pape, Kristin, 2008, Finding concealed active faults—Extending the southern Whidbey Island fault across the Puget Lowland, Washington: Journal of Geophysical Research, v. 113, B05313, doi:10.1029/2007JB005060, 2008.

Squires, R. L.; Goedert, J. L.; Kaler, K. L., 1992, Paleontology and stratigraphy of Eocene rocks at Pulali Point, Jefferson County, eastern Olympic Peninsula, Washington: Washington Division of Geology and Earth Resources Report of Investigations 31, 27 p. [http://www.dnr.wa.gov/publications/ger_ri31_eocene_rock_jefferson_county.pdf]

Tabor, R. W.; Cady, W. M., 1978, Geologic map of the Olympic Peninsula, Washington: U.S. Geological Survey Miscellaneous Investigations Series Map I-994, 2 sheets, scale 1:125,000.

Tabor, R. W.; Haugerud, R. A.; Haeussler, P. J.; Clark, K. P., 2011, Lidar-revised geologic map of the Wildcat Lake 7.5′ quadrangle, Kitsap and Mason Counties, Washington: U.S. Geological Survey Scientific Investigations Map 3187, 2 sheets, scale 1:24,000, with 12 p. text. [http://pubs.usgs.gov/sim/3187]

Thackray, G. D., 2001, Extensive early and middle Wisconsin glaciation on the western Olympic Peninsula, Washington, and the variability of Pacific moisture delivery to the northwestern United States: Quaternary Research, v. 55, no. 3, p. 257-270.

Thackray, G. D.; Rittenour, T. M., 2012, New OSL ages and revised stratigraphic and geomorphic evolution of the Olympic coast of Washington, USA, during the last glacial cycle [abstract]. *In* American Quaternary Association Program and abstracts of the 21st bienniel meeting of the American Quaternary Association—AMQUA 2010: American Quaternary Association, p. 106. [http://www.cce.umn.edu/Documents/CPE-Conferences/2012AMQUAProgramAbstractsBook.pdf]

Thorson, R. M., 1981, Isostatic effects of the last glaciation in the Puget Lowland, Washington: U.S. Geological Survey Open-File Report 81-370, 100 p., 1 plate. [http://pubs.er.usgs.gov/publication/ofr81370]

Thorson, R. M., 1989, Glacio-isostatic response of the Puget Sound area, Washington: Geological Society of America Bulletin, v. 101, no. 9, p. 1163-1174.

Troost, K. G.; Booth, D. B., 2008, Geology of Seattle and the Seattle area, Washington. *In* Baum, R. L.; Godt, J. W.; Highland, L. M., editors, Landslides and engineering geology of the Seattle, Washington, area: Geological Society of America Reviews in Engineering Geology XX, p. 1-35. [http://www.wou.edu/las/physci/taylor/g473/seismic_hazards/troost_booth_2008_geo_seattle.pdf]

Troost, K. G.; Booth, D. B.; Mahan, S. A.; Hagstrum, J. T., 2003, Presence of mid-Pleistocene deposits (MIS 4 through 8) in the Tacoma area—Did the Possession glacier make it to Tacoma? [abstract]: Geological Society of America Abstracts with Programs, v. 35, no. 6, p. 215.

U.S. Geological Survey Geologic Names Committee, 2010, Divisions of geologic time—Major chronostratigraphic and geochronologic units: U.S. Geological Survey Fact Sheet 2010-3059, 2 p. [http://pubs.usgs.gov/fs/2010/3059/]

Van Wagoner, T. M.; Crosson, R. S.; Creager, K. C.; Medema, G. F.; Preston, L. A.; Symons, N. P.; Brocher, T. M., 2002, Crustal structure and relocated earthquakes in the Puget Lowland, Washington, from high-resolution seismic tomography: Journal of Geophysical Research, v. 107, no. B12, 2381, DOI:10.1029/20012JB000710, p. ESE 22-1–22-23.

Waitt, R. B., Jr.; Thorson, R. M., 1983, The Cordilleran ice sheet in Washington, Idaho, and Montana. *In* Porter, S. C., editor, The late Pleistocene; Volume 1 *of* Wright, H. E., Jr., editor, Late-Quaternary environments of the United States: University of Minnesota Press, p. 53-70.

Yount, J. C.; Gower, H. D., 1991, Bedrock geologic map of the Seattle 30′ by 60′ quadrangle, Washington: U.S. Geological Survey Open-File Report 91-147, 37 p., 4 plates. [http://pubs.er.usgs.gov/publication/ofr91147]

Yount, J. C.; Minard, J. P.; Dembroff, G. R., 1993, Geologic map of surficial deposits in the Seattle 30' x 60' quadrangle, Washington: U.S. Geological Survey Open-File Report 93-233, 2 sheets, scale 1:100,000. [http://ngmdb.usgs.gov/Prodesc/proddesc_12654.htm]

Zdanowicz, C. M.; Zielinski, G. A.; Germani, M. S., 1999, Mount Mazama eruption—Calendrical age verified and atmospheric impact assessed: Geology, v. 27, no. 7, p. 621-624.

Appendix A. Bedrock Elevation Estimates from Passive Seismic Survey Data

Passive seismic measurements for determining depth to bedrock were made with a Tromino device (spectral range of 0.1 to 128 Hz) at all seismic sites. A Güralp device (spectral range of 0.03 to 100 Hz) was additionally used at one site as noted. We also employed a 12-channel microtremor array with 4.5-Hz sensors for passive seismic measurements to determine shear wave velocity at depths less than about 330 ft below the surface at some sites as noted. We used a formula from Kramer (1996; see also Lane and others, 2008) to infer depth to bedrock: depth = Vs/(4*(fr)), where Vs is the mean shear-wave velocity (m/s) in the deposits above the estimated depth, and fr (Hz) is the resonant frequency corresponding to peak horizontal-to-vertical spectral ratio (HVSR). We determined Vs values for unconsolidated deposits between 116 and 980 m/s by using Tromino Grilla® software to model HVSR data, calibrated by our microtremor array measurements. We judged our values to be similar in sediments at all sites.

Table A1. Bedrock elevation estimates. Sites are shown on map. Latitude and longitude coordinates were generated from sample locations as plotted in ArcGIS (projection Washington State Plane South, NAD 83 HARN, U.S. Survey feet). Elevations are in feet, estimated using Puget Sound Lidar Consortium lidar grid elevations (vertical datum NAVD88, projected to Washington State Plane South, NAD 83 HARN, U.S. Survey feet). Lidar elevation statements differ from elevations implied by the base map and were used because we believe them to be more accurate. They were not adjusted to account for projection differences relative to the base map (vertical datum NGVD 29). Lidar level 0 theoretically is 3.51 to 3.59 ft below base map level 0 [http://www.ngs.noaa.gov/cgi-bin/VERTCON/vert_con.prl]. Shear-wave velocity estimates for sediments were obtained by modeling H/V spectral data (Micromed s.p.a., 2012) for depths of less than1,640 ft. These estimates were not checked against gravity and (or) magnetic modeling. Site HVSR5 (*) is included in both a north–south and an east–west transect across the Kitsap Peninsula and is therefore listed twice in the table below.

Seismic site	TRS	Lat./ long. (degrees)	Elevation (ft)	Sediment Vs (m/s)	Bedrock depth estimate (ft)	Bedrock elevation estimate (ft)	Notes
Transect from west to east across the Kitsap Peninsula in the Brinnon, Seabeck, and Poulsbo quadrangles (see also cross section A–A′–A″)							
HVSRx	sec. 25, T25N R2W	47.63123 -122.88123	13	400	1,600	-1,587	Previous result from survey site 2,360 ft north and 1,220 ft west of the southwest corner of the map area (Brinnon quadrangle; Polenz and others, 2012c). Estimate assumes uniform sediment shear wave velocity and thereby employs a simpler model than at other sites.
HVSR1	sec. 30, T25N R1W	47.63448 -122.84511	324	129-750	>1,640	<-1,316	Model suggests gradual seismic velocity increase with depth and lacks clear indication of a bedrock contact.
HVSR2	sec. 21, T25N R1W	47.63939 -122.81383	328	196-681	>1,640	<-1,312	Model suggests gradual seismic velocity increase with depth and lacks clear indication of a bedrock contact.
HVSR3	sec. 15, T25N R1W	47.65597 -122.78770	15	203-528	>1,640	<-1,625	Model suggests gradual seismic velocity increase with depth and lacks clear indication of a bedrock contact.
HVSR4	sec. 13, T25N R1W	47.65984 -122.75473	58	193-860	3,370	-3,312	Range of bedrock elevation estimates was -1,248 to -5,508 ft; shear wave velocity Vs of bedrock determined by modeling was 1,500 m/s below a depth of 1,286 ft corresponding to a spectral ratio of 3.22.
HVSR5*	sec. 18, T25N R1E	47.65875 -122.71604	324	270-980	2,850	-2,526	Near-surface (<330 ft depth) shear wave velocity Vs of about 550 m/s was measured using a 12-channel passive seismic array. Range of bedrock elevation estimates was -1,706 to -3,346 ft; shear wave velocity Vs of bedrock determined by modeling was 1,600 m/s (or more) below a depth of 2,848 ft (±820 ft) corresponding to a spectral ratio of 0.28. This seismic site was also part of a transect from south to north along the Kitsap Peninsula (see below).
HVSR6	sec. 15, T25N R1E	47.65775 -122.66849	287	141-754	>1,640	<-1,353	Model suggests gradual seismic velocity increase with depth and lacks clear indication of a bedrock contact.
HVSR7	sec. 14, T25N R1E	47.65228 -122.63962	80	116-850	>1,640	<-1,560	Passive seismic measurements made with a Güralp device were used to determine depth to bedrock; measurements by Tromino device were similar. Model

Seismic site	TRS	Lat./ long. (degrees)	Elevation (ft)	Sediment Vs (m/s)	Bedrock depth estimate (ft)	Bedrock elevation estimate (ft)	Notes
							suggests gradual seismic velocity increase with depth and lacks clear indication of a bedrock contact.
Transect from south to north along the Kitsap Peninsula in the Poulsbo quadrangle							
HVSR8	sec. 19, T25N R1E	47.63714 -122.72579	528	109-661	>1,640	<-1,112	Model suggests gradual seismic velocity increase with depth and lacks clear indication of a bedrock contact.
HVSR5*	sec. 18, T25N R1E	47.65875 -122.71604	324	270-980	2,850	-2,526	Near-surface (<330 ft depth) shear wave velocity Vs of about 550 m/s was measured using a 12-channel passive seismic array. Range of bedrock elevation estimates was -1,706 to -3,346 ft; shear wave velocity Vs of bedrock determined by modeling was 1600 m/s (or more) below a depth of 2,848 ft (±820 ft) corresponding to a spectral ratio of 0.28. This seismic site was also part of a transect from west to east across the Kitsap Peninsula (see above).
HVSR9	sec. 5, T25N R1E	47.69392 -122.69875	252	129-722	>1,640	<-1,388	Model suggests gradual seismic velocity increase with depth and lacks clear indication of a bedrock contact.
HVSR10	sec. 28, T26N R1E	47.74910 -122.68918	407	154-500	>1,640	<-1,233	Model suggests gradual seismic velocity increase with depth and lacks clear indication of a bedrock contact.
HVSR11	sec. 16, T26N R1E	47.74971 -122.68825	419	220-980	>1,640	<-1,221	Near-surface (<330 ft depth) shear wave velocity of about 500 m/s was measured using a 12-channel passive seismic array. Model suggests gradual seismic velocity increase with depth and lacks clear indication of a bedrock contact.
Transect from south to north along the Toandos Peninsula in the Seabeck quadrangle (see cross section B–B′)							
HVSR12	sec. 15 T26N R1W	47.44597 -122.47689	495	145-579	2,103	-1,608	Near-surface (<302 ft depth) shear wave velocity Vs of about 584 m/s was measured using a 12-channel passive seismic array. Shear wave velocity Vs of bedrock determined by modeling was 1,272 m/s below a depth of 2,103 ft corresponding to a spectral ratio of 0.19.
HVSR13	sec. 22, T26N R1W	47.43756 -122.47765	443	– – –	– – –	– – –	Near-surface (<302 ft depth) shear wave velocity of about 939 m/s was measured using a 12-channel passive seismic array. Tromino measurements yielded no usable data. Tromino was therefore moved to site HVSR14 (1,150 ft from HVSR13).
HVSR14	sec. 21, T26N R1W	47.43849 -122.48011	410	180-630	3,710	-3,300	Shear wave velocity Vs of bedrock determined by modeling was 1,150 m/s below a depth of 3,710 ft corresponding to a spectral ratio of 0.19.
HVSR15	sec. 27, T26N R1W	47.42985 -122.47855	400	198-720	4,685	-4,285	Shear wave velocity Vs of bedrock determined by modeling was 1,374 m/s below a depth of 4,685 ft corresponding to a spectral ratio of 0.22.
HVSR16	sec. 33, T26N R1W	47.42055 -122.48382	208	226-827	2,805	-2,597	Shear wave velocity Vs of bedrock determined by modeling was 1,573 m/s below a depth of 2,805 ft corresponding to a spectral ratio of 0.19.

Appendix B. New Radiocarbon and Luminescence Dates

Table B1. Radiocarbon age-control data from the map area. All dates are previously unpublished, except for a 16,510 ±320 ^{14}C yr BP radiocarbon date on wood from below Vashon Drift at date site GD7 (sec. 21, T25N R1E)(Fig. D4; see also *Description of Map Units*, p. 11; *Vashon Drift*, p. 14; Deeter, 1979, UW 446; excluded from table below). Conventional (^{14}C) "Radiometric Plus" radiocarbon analyses by Beta Analytic, Inc. Atomic mass spectrometry (AMS) radiocarbon analyses by Direct AMS, Accium BioSciences, Inc. Sites are shown on map. Latitude and longitude coordinates were generated from sample locations as plotted in ArcGIS (projection Washington State Plane South, NAD 83 HARN, U.S. Survey feet). Elevations are in feet, estimated using Puget Sound Lidar Consortium lidar (vertical datum NAVD88, projected to Washington State Plane South, NAD 83 HARN, U.S. Survey feet) supplemented on bluffs by visual elevation estimates. The lidar-based elevation statements were not adjusted to account for projection differences relative to the base map (vertical datum NGVD 29)—lidar level 0 theoretically is 3.51–3.59 ft below base map level 0 [http://www.ngs.noaa.gov/cgi-bin/VERTCON/vert_con.prl]. Geologic units are the interpretation of this study for the sample host material. Age estimates in radiocarbon years before 1950 (^{14}C yr BP) are reported with one standard deviation of uncertainty (1σ = 68% confidence interval) and are 'conventional' (adjusted for measured ^{13}C/^{12}C ratio). Age estimates stated in ka are in calendar years before 1950 divided by 1000 and are reported with two standard deviations of uncertainty (2σ = 95% confidence interval) as reported by Beta Analytic Inc., or, for Direct AMS samples, as calculated using OxCal online [http://c14.arch.ox.ac.uk/embed.php?File=oxcal.html]. Uncertainty statements reflect random and lab errors; errors from unrecognized sample characteristics or flawed methodological assumptions (for example, ^{14}C sample contamination from younger carbon flux) are not known.

Date site	Field sample ID	Lab sample ID	Site name	TRS	Lat./ long. (degrees)	Elev. (ft)	Map unit	Material dated	Analytic method	^{13}C/^{12}C (o/oo)	Age estimate	Notes
Kitsap County dates (east of Hood Canal)												
GD1	12-54-M-0608-c	Beta 338914	Dyes Inlet beach	sec. 21, T25N R1E	47.64434 -122.68083	6	Qm	wood	^{14}C	-21.3	1,240 ±30 ^{14}C yr BP (1.270-1.070 ka)	Root segment with ~48 root growth rings (and bark, which was excluded from analysis), from a stump identified by Rex Crawford (DNR Natural Heritage Program) as western redcedar (*Thuja plicata*). The sample and at least one stump of an unidentified species are rooted in growth position in a relict peat mat exposed along the shore of Dyes Inlet (Fig. D1). Both peat layers are exposed in the intertidal zone and are being eroded by beach retreat along the east shore of Dyes Inlet. The *Thuja plicata* root sample was collected about 5 ft from the center of the stump and was intertwined with other roots and more delicate fibrous plant matter. Stump dimensions and wood-to-root growth pattern suggest a larger (and thus older) tree. We sampled root because it was well-preserved, with bark, whereas the stem was eroded and lacked bark. The sample weighed ~180 g (dry, including bark, which was excluded from analysis). A T-sheet coastal survey (AD 1880) suggests that a coastal wetland was present in the late 1800s. The sample was collected about 3.6 ft below the level of the modern inland marsh surface (Fig. D1).
GD2	12-65-M-0719c	Beta 339541	eastern tributary to Anderson Creek	sec. 13, T25N R1E	47.66376 -122.74461	200	Qapo	peat (plant debris)	^{14}C	-27.2	>43,500 ^{14}C yr BP	Plant debris from a few feet of laminated silt with peaty debris, exposed midway in a section of laminated silt and pebble gravel; basal peat selected for analysis to avoid possible up-section contamination by modern carbon. Pollen analysis yielded too few pollen grains for paleoenvironmental interpretation (Leopold, written and oral commun., 2013).

Date site	Field sample ID	Lab sample ID	Site name	TRS	Lat./ long. (degrees)	Elev. (ft)	Map unit	Material dated	Analytic method	$^{13}C/^{12}C$ (o/oo)	Age estimate	Notes
GD3	12-77-M-0851b	Beta 335694	unnamed drainage west of Silverdale	sec. 18, T25N R1E	47.65323 -122.71484	220	Qpos	delicate plant debris	^{14}C	-28.7	>43,500 ^{14}C yr BP	Delicate plant debris (reed-like stems, seeds, small wood) from laminated silt near base of upward-coarsening section of silt (base) to sand to pebble gravel (top), all beneath surficial till. Sediment contains almost no pollen, only a few pine, alder, and birch (Leopold, written and oral commun., 2013).
Jefferson County dates (Toandos Peninsula and north of Jackson Cove)												
GD8	41-C-21-B	Beta 335224	Camp Parson	sec. 13, T26N R2W	47.44965 -122.52216	301	Qgic	charred wood	AMS	-23.7	1,640 ±30 ^{14}C yr BP (1.600-1.580 ka, 1.570-1.510 ka, 1.460-1.440 ka, and 1.430-1.420 ka)	Charred wood from postulated forest fire event sampled in road bed at Camp Parsons.
GD9	42-C-38-C	D-AMS 1547	Tabook Point terrace	sec 16, T26N R1W	47.44962 -122.48459	10	Qoa	wood	AMS	-25.0	1,349 ±32 ^{14}C yr BP (1.318-1.181 ka)	Organic debris exposed in a flat terrace perched 3 ft above the modern beach. Upright old-growth tree stumps confirm the prehistoric terrace age suggested by the radiocarbon analysis.
GD12	K-610-A	Beta 338310	Walton terrace	sec. 28, T26N R1W	47.43373 -122.49429	54	Qoa	charred material	AMS	-23.8	2,010 ±30 ^{14}C yr BP (2.040-2.030 ka, and 2.000-1.890 ka)	Detrital charcoal found at stream level under a 20-ft-thick alluvial terrace. The organics were deposited in a gray silt and sand layer under 12 to 20 ft of sandy pebble gravel (alluvium). Upright old growth tree stumps on top of the terrace confirm the prehistoric terrace age suggested by the radiocarbon analysis. Stream incision documents subsequent terrace abandonment.
GD13	57-K-579-A	D-AMS 1548	drainage south of fault exposure	sec. 28, T26N R1W	47.42977 -122.48595	159	Qc_o	gyttja	AMS	-23.3	>45,000 ^{14}C yr BP	Gyttja (peat, reeds, or wood fragments) deposited in silt and sand layer between beds of Olympic-sourced sand and pebble gravels. Pollen analysis yielded too few pollen grains for paleoenvironmental interpretation (Leopold, written and oral commun., 2013). Lab comments that the sample is too old to be reliably dated by the AMS method.
GD14	54-K-515-B	Beta 341759	Fisherman's Harbor	sec. 4, T25N R1W	47.41372 -122.48187	33	Qc_o	various organics	AMS	-27.7	35,210 ±320 ^{14}C yr BP (41.100-39.440 ka)	Undifferentiated organics found within a paleosol formed on gray silt, sand, and sandy pebble gravel with brown alpine outwash above.

Table B2. Infrared and optically stimulated luminescence age-control results from the map area. All dates are previously unpublished. Optically stimulated luminescence (OSL) analysis and infrared stimulated luminescence (IRSL) analysis by Shannon Mahan, U.S. Geological Survey. Analytical data are provided in Table B3. Sites are shown on map. Latitude and longitude coordinates were generated from sample locations as plotted in ArcGIS (projection Washington State Plane South, NAD 83 HARN, U.S. Survey feet). Elevations are in feet, estimated using Puget Sound Lidar Consortium lidar grid elevations (vertical datum NAVD88, projected to Washington State Plane South, NAD 83 HARN, U.S. Survey feet) supplemented on bluffs by visual elevation estimates. The lidar-based elevation statements were not adjusted to account for projection differences relative to the base map (vertical datum NGVD 29). Lidar level 0 theoretically is 3.51 to 3.59 ft below base map level 0 [http://www.ngs.noaa.gov/cgi-bin/VERTCON/vert_con.prl]. Geologic units are the interpretation of this study for the sample host material. Uncertainty values of age estimate ranges reported span one standard deviation (1σ = 68% confidence interval). Uncertainty statements reflect random and lab errors; errors from unrecognized sample characteristics or flawed methodological assumptions (for example, incomplete pre-depositional re-setting of luminescence samples) are not known.

Date site	Field/ lab sample ID	Site name	TRS	Lat./ Long. (degrees)	Elev. (ft)	Map unit	Material dated	Analytic method	Age estimate	Notes
Kitsap County dates (east of Hood Canal)										
GD4	12-63-M-0706	unnamed drainage west of Dyes Inlet at southern map edge	sec. 30, T25N R1E	47.62482 -122.71637	202	Qga_p	sand	IRSL	103.620 ±6.270 ka	Gently crossbedded, medium sand of northern or Cascade provenance (see also Description of map units section, unit Qga_p, capped ~20 to 40 ft above the sample by a well-developed pre-Vashon till of northern provenance. A tally of 39 pebbles (sparsely disseminated within the sand) revealed 19 basalt (49%), 6 granitic (15%), 4 chert (10%), 3 sandstone (8%), 2 gabbro or diorite (5%), 1 porphyritic (3%), and 4 unidentified (10%) clasts. Except for 5 rotten basalt clasts, all clasts were substantially unweathered. Lab comments that divergent OSL and IRSL results are indicative of partial bleaching and suggest that deposits are younger than the stated 103 ka IRSL age.
								OSL	>40.000 ka	
GD5	12-65-M-0723a	eastern tributary to Anderson Creek	sec. 13, T25N R1W	47.66209 -122.74720	150	Qga_p	sand	IRSL	97.250 ±4.850 ka	Planar-bedded, compact, clean, fine sand of either Cascade or northern provenance that may have incorporated reworked sediment of Cascade provenance (see unit Qga_p). Overlies till, the base of which was observed 9 to 10 ft lower in the section. The till directly contacted and incorporated peat found immediately below. The peat yielded insufficient pollen for paleoenvironmental interpretation (Leopold, written and oral commun., 2013). Lab comments that failure to yield OSL results suggests partial bleaching and that deposits are younger than the stated 97 ka IRSL age.
GD6	12-64-M-0714	shore bluff east of Hood Canal	sec. 12, T25N R1W	47.67494 -122.74818	~80	Qpos	sand	IRSL	>185.000 ka	Planar to gently crossbedded medium sand with thin interbeds of pebbles. Pebble lithology is dominated by sandstone (45%, based on count of 42 clasts) and includes diverse lithologies hinting at a northern source. Overlain by gravel with dominantly basalt (43%, based on count of 49 clasts) and sandstone (37%) clasts, and by surficial Vashon till. Underlain by dense silty sandy gravel dominated by Olympic-derived lithologies. Site elevation estimate approximate, between ~ 75 and 95 ft.
GD15	12-62-M-0702c	sand pit at Asbury's Topsoil	sec. 25, T25N R1W	47.63298 -122.74190	341	Qgos	sand	IRSL	17.130 ±1.080 ka	Planar to gently crossbedded, compact, silty, very fine sand. Overlain by ~30 ft of rhythmically bedded very fine clast-free sand in thick (~1 ft) packages (varves?) that appear to be draped over the topography (deposits of Glacial Lake Russell or an associated slow-moving channel?). Bedding structure more complex at base of sequence at the sampling location in subpit.
								OSL	16.580 ±1.140 ka	

Table B3. Luminescence analytical data for age-control results from the map area. This table provides elemental concentrations, cosmic and total dose rates, equivalent doses, and ages from IRSL (fine feldspars) and OSL (quartz). Detailed sample descriptions are provided in Table B2. Errors to 1σ. For field water content, figures in parentheses indicate the complete sample saturation (%). Ages calculated using approximately 60 percent of saturation values. Analyses of potassium (K), uranium (U), and thorium (Th) obtained using a high resolution Germanium detector on a laboratory gamma ray spectrometer. Cosmic doses and attenuation with depth were calculated using methods of Prescott and Hutton (1994). Figures in parentheses indicate total number of measurements made, including failed runs with unusable data; Gy, unit of absorbed radiation in Grays; n, number of replicated equivalent dose (De) estimates used to calculate the mean. Dose rate and OSL age for quartz from fine-grained 250–180-micron sand. Linear + exponential fit used on equivalent dose, with single aliquot regeneration. Dose rate and IRSL age for feldspar from fine silt grains of 4–11-micron polymineral silt. Exponential fit used for multiple aliquot additive doses. Fade tests indicate no correction.

Date site	Field/Lab sample ID	Water content* (%)	K (%)	U (ppm)	Th (ppm)	Cosmic dose additions (Gy/ka)	Total dose rate (Gy/ka)	Equivalent dose (Gy)	n*	Analytic method	Age estimate
GD4	12-63-M-0706	4 (18)	2.20 ±0.05	1.17 ±0.16	5.80 ±0.62	0.11 ±0.01	3.59 ±0.20	372 ±8.56	– – –	IRSL	103.620 ±6.270 ka
							2.74 ±0.15	>110	15 (17)	OSL	>40.000 ka
GD5	12-65-M-0723a	7 (24)	2.41 ±0.05	1.80 ±0.17	6.03 ±0.55	0.11 ±0.01	3.64 ±0.16	354 ±11.0	– – –	IRSL	97.250 ±4.850 ka
GD6	12-64-M-0714	12 (21)	2.15 ±0.05	1.43 ±0.14	5.53 ±0.41	0.10 ±0.01	3.54 ±0.14	>650	– – –	IRSL	>185.000 ka
GD15	12-62-M-0702c	21 (39)	0.98 ±0.04	1.00 ±0.13	3.19 ±0.32	0.07 ±0.01	1.71 ±0.10	29.3 ±0.79	– – –	IRSL	17,130 ±1,080 ka
							1.24 ±0.07	20.6 ±0.78	21 (28)	OSL	16,580 ±1,140 ka

Appendix C. New Tephra Data from Geochemistry Site G1

Table C1. New electron microprobe geochemical data on tephra at geochemistry site G1 (unit Qoa). The tephra was sampled from a relict stream terrace at the site (sec. 8, T25N R1E; longitude 122.69734°, latitude 47.67488°) and provides an excellent match to glass found in the Mazama tephra. Based on analysis of 16 shards, the sample has a similarity coefficient (Borchardt and others, 1972) of 0.98+ to a Mazama climactic standard tephra and even more closely resembles other tephras thought to be Mazama (similarity coefficients up to 0.993)(Franklin Foit, Wash. State Univ., written commun., 2012). Foit noted that sample does not appear to contain traces of other tephras and advocated a tephra age of 6,730 ±40 ^{14}C yr BP, as published by Hallet and others (1997), and equivalent to the 7,627 ±150 cal yr BP estimate published by Zdanowicz and others (1999). Foit (written commun., 2013) reported a 96.11 weight percent microprobe analytical total, equivalent to 3.89 percent loss on ignition.

Oxide	Percent (normalized)	Standard deviation
SiO_2	72.84	0.2
$A1_2O_3$	14.68	0.17
Fe_2O_3	2.04	0.05
TiO_2	0.43	0.04
Na_2O	5.01	0.2
K_2O	2.75	0.08
MgO	0.45	0.03
CaO	1.58	0.07
Cl	0.22	0.05
Total	100	– – –

Appendix D. Illustrations of Selected Field Sites

Figure D1. Relict peat and tree stump at date site GD1 (east shore of Dyes Inlet, sec. 21, T25N R1E). A western redcedar stump (Inset A)(Table B1) and at least one stump of an unidentified species 40 ft north are rooted in growth position in a relict peaty marsh mat (brown beach substrate around date site GD1) with a dense tree root network in a matrix of woody and more delicate fibrous plant matter and organic mud. The peat is overlain by 6 to 8 in. of more recent peat consisting of mostly delicate fibrous plant matter and organic mud (but lacking the web of in-place tree roots observed in the lower peat). The root sample (Inset B) was collected at an elevation of about 6 ft (determined by lidar; see Appendix B), about 6 to 6.5 ft below the crest of the modern, pebbly beach-top berm (with a crest elevation from 11–13 ft). The sample was thus collected about 3.6 ft below the level of the modern marsh surface inland of the beach.

Figure D2. Rhythmically bedded, very fine sand of unit Qgos, with slump structures in the main pit wall of Asbury's Topsoil sand pit (date site GD15, sec. 13, T25N R1W). A sand sample for luminescence analysis by IRSL and OSL (Tables B2 and B3) was collected in a subpit of the main pit floor (*top left*). The pit wall exposes approximately 20 1-ft-thick rhythmites (varves?). We interpret the bench above the main pit wall as an early shoreline of Lake Russell at elevation 420 to 400 ft. The level of the main pit floor is lateral to a later channel carved into the bench at elevation 380 to 360 ft. The sample was collected at the bottom of the subpit about 10 ft below the main pit floor and thus below approximately 30 rhythmites at an elevation of about 340 ft.

Figure D3. Planar to gently crossbedded, clean, medium sand with pebble lenses of unit Qga_p in the cutbank of a ravine at date site GD4 (sec. 30, T25N R1E) along the southern edge of the Poulsbo quadrangle west of Dyes Inlet. This thick sand of northern or Cascade (Snohomish River basin?) provenance is exposed below a well-developed pre-Vashon northern-sourced till (unit Qgt_p) at elevation 202 ft. Collection of a sand sample for luminescence analysis by IRSL and OSL (Tables B2 and B3) is shown in progress.

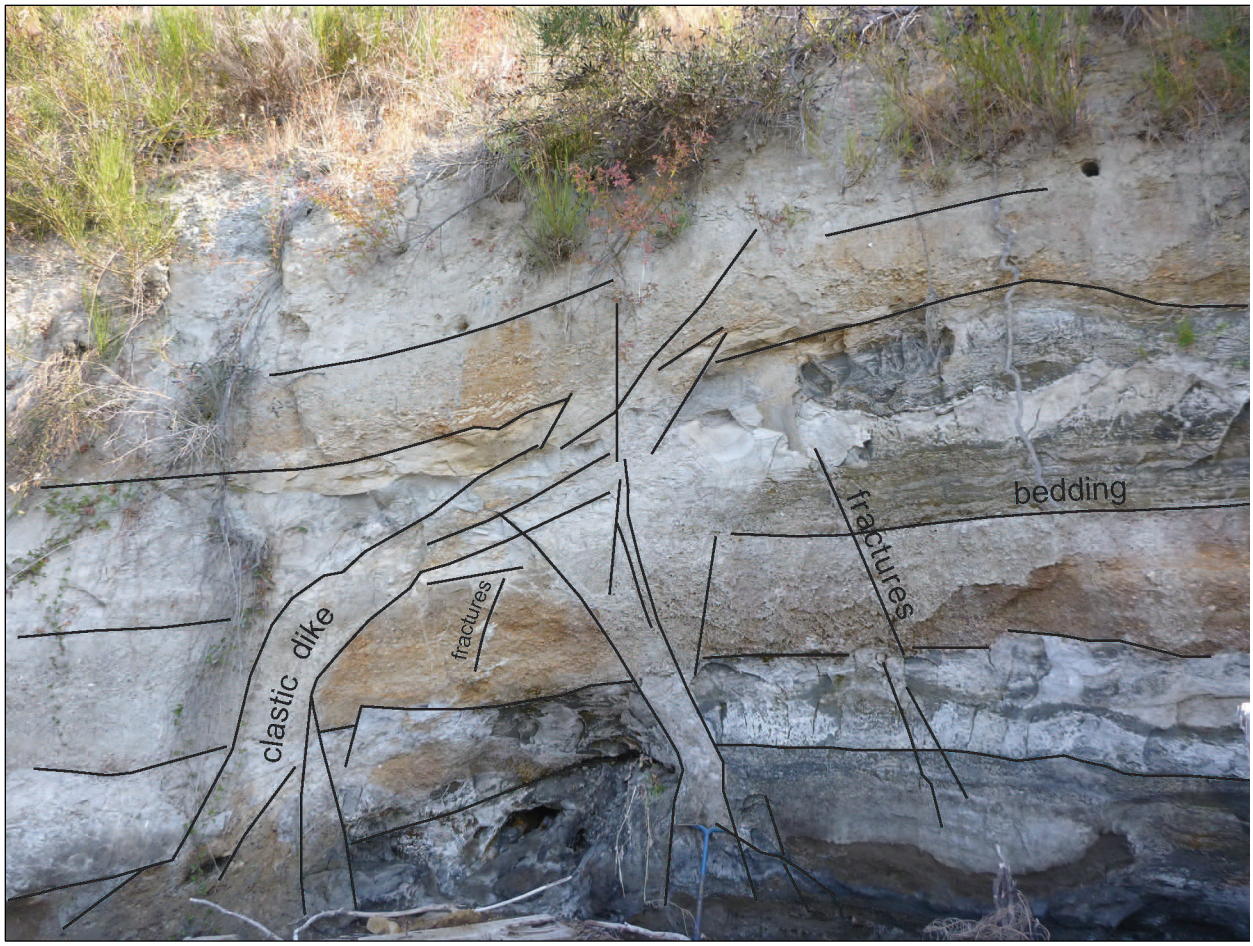

Figure D4. Gently folded and fractured, planar-bedded, pebbly sand and silt of unit Qc_O along a bluff on the east shore of Dyes Inlet just north of radiocarbon age site GD7 (sec. 21, T25N R1E). The structure is a north-side-down step defined by warped and fractured bedding with clastic dike injection features. The fractures and clastic dikes dip steeply north or south with strikes of about 200 to 210° and 90 to 100°, respectively. The anticlinal fold on the south (axis trend 288°, plunge 4°), combined with an upright syncline on the north, results in a total north-side-down monoclinal step of about 3 ft. Proximal panels of planar strata to the north and south of this structure dip gently 3–5° ESE and are delimited distally by similar fold and fracture structures. The sourced of the strata is distinctly Olympic with pebbles of primarily sandstone and basalt and little diversity beyond a few bits of vein quartz. Organic silt at the base of the section is interbedded with dark-gray medium sand that includes flattened sticks with a 16,510 ±320 ^{14}C yr BP radiocarbon date by Deeter (1979)(see text, unit Qc_O). View is looking east. The bluff is approximately 15 ft high with a 65-cm geologist's pick shown for scale.